THE EFFECT OF ACUTE AND CHRONIC THERMOTHERAPY ON TYPE 2 DIABETIC SKELETAL MUSCLE GENE EXPRESSION AND INFLAMMATORY RESPONSES

A Thesis

by

LOUAY Z. BACHNAK

BS, University of Texas Rio Grande Valley, 2017

Submitted in Partial Fulfillment of the Requirements for the Degree of

MASTER OF SCIENCE

in

BIOLOGY

Texas A&M University-Corpus Christi
Corpus Christi, Texas

August 2020

August 2020

THE EFFECT OF ACUTE AND CHRONIC THERMOTHERAPY ON TYPE 2 DIABETIC SKELETAL MUSCLE GENE EXPRESSION AND INFLAMMATORY RESPONSES

A Thesis

by

LOUAY Z. BACHNAK

This thesis meets the standards for scope and quality of
Texas A&M University-Corpus Christi and is hereby approved.

Felix Omoruyi, PhD
Chair

Jean Sparks, PhD
Co-Chair

Xavier Gonzales, PhD
Committee Member

Daniel Newmire, PhD
Committee Member

August 2020

ABSTRACT

Diabetes is a complex chronic illness associated with a state of high blood glucose level occurring from deficiencies in insulin secretion, action, or both. The disease affects millions of people globally. Type 2 Diabetes is associated with insulin resistance or a defective secretion of insulin from the pancreas. The skeletal muscle system accounts for 80% of glucose uptake and is a vital player in healthy aging and muscle mass maintenance. This muscle system also adapts to various stimuli, which are interdependent to fiber-type distribution, metabolism, and changes in muscle size. **PURPOSE:** The purpose of this study was to investigate the effects of thermotherapy on skeletal muscle metabolism, with an emphasis on gene expression, inflammation, and cell viability, in Type 2 Diabetic skeletal muscle. **METHODS:** Human skeletal muscle myoblast (HSMM) and Diabetic Type 2 human skeletal muscle myoblast (D-HSMM) (Lonza Inc, Walkersville, MD) cells were cultured until 70% confluency was reached, and then subjected to heat treatment – acute or chronic. The chronic heat treatment consisted of a 30-minute exposure to 40°C, three times a week for three weeks, while the acute heat treatment consisted of a one-time exposure to 40°C for 30 minutes. Approximately, 10^5 cells of each cell type (HSMM and D-HSMM), along with growth media, were seeded into 24-well plates for a total volume of 2 mL per well. Groups included control cells (CON), chronic treatment (CH), and acute treatment (AC). Following a 48-hour incubation period, the chronic treatment was initiated, while the acute treatment was performed during the last session of the chronic treatment. Following the treatments, cell viability and density were determined. The cDNA was isolated and a real-time polymerase chain reaction (QuantStudio 3 Real-time PCR Instrument, Thermofisher, Waltham, MS) was performed to assess an array of gene expression. To assess inflammation, ELISA was performed on cytokines Interleukin 1β, IL-4, IL-6, IL-10, and tumor necrosis factor (TNF) -α. **RESULTS:**

There was significant evidence supporting a difference between cell viability percentage following the acute thermotherapy ($p = 0.0006$) on D-HSMM, however, no significant change occurred in chronic thermotherapy. Through a qualitative assessment of gene expression, HSMM yielded the highest elevations under the chronic treatment compared to the control - AcvR2B (215.613-fold), IGF-2 (59.063-fold), and CTNNB1 (47.492-fold). Similarly, in D-HSMM cells, chronic heat treatment yielded an up-regulation of IGF-2 (0.485-fold), TNNT3 (0.399-fold), and PGC1B (0.328-fold), while in the acute treatment, an up-regulation of ACTB (1.648-fold) was observed. Acute and chronic heat treatments of HSMM cells significantly down-regulated IL-1β, IL-6, IL-10, and TNF-α. Acute heat treatment of D-HSMM cells resulted in a significant decrease in IL-1β, IL-6, and up-regulation of IL-10 and TNF-α levels. In contrast, chronic treatment yielded a reduction in IL-4, TNF-α, and an up-regulation of IL-6 and IL-10 levels. **CONCLUSION**: The results suggest an increase in gene expression is related to actin activity (ACTB), sarcolemma repair (SGCA), and cellular responses (IGFBP3, CTNNB1, TNNT3), which could be indicative of an increase in transcriptional regulation. The observed increase in ACTB may indicate an increase in the regulation of energy balance due to the environmental change in both treatments. A significant difference is evident between acute treatment and control regarding cell viability percentage. In D-HSMM, proinflammatory cytokine IL-6 was seen upregulated following the chronic treatment, along with IL-10. This significant upregulation was negatively correlated with a decrease in TNF-α and IL-1β, which may be indicative of improved adverse inflammatory effects associated with the diabetic population.

Key Words: heat stress, type 2 diabetes, skeletal muscle cells, gene expression, thermotherapy

DEDICATION

This work is dedicated to my wonderful family and friends who continue to be sources of inspiration, support, encouragement, and unconditional love. While this journey was an intense undertaking, they made it bearable and enjoyable.

ACKNOWLEDGEMENTS

I would like to acknowledge this project could not have been done without the assistance from various mentors, family, and friends whose support was vital to this study, and my academic and personal success.

I am eternally grateful for my graduate advising committee who dedicated their time to support and mentor me, and for their patience on this journey. To my Chair and co-Chair of the advisory committee, I am deeply grateful to Dr. Felix Omoruyi and Dr. Jean Sparks for accepting me as a graduate student in their lab and volunteering to guide me throughout this program. I would like to thank Dr. Omoruyi for his valuable support in guiding me throughout the program and ensuring I stayed on track for graduation. I appreciate his inspiration in making me more confident by taking challenging opportunities in my academic life. I would also like to thank Dr. Sparks for her tenderness and continued support along this journey. I appreciate her patience in editing my papers and for always having her door open for any problems that arose.

I would also like to thank my other committee members Drs. Xavier Gonzales and Daniel Newmire. I would like to thank them for their continued support. I appreciate Dr. Gonzales's guidance throughout this project and expertise in the field. I appreciate the support of Dr. Newmire for always making sure I was up to date on new publications, analyzing my data, and continued support throughout the two years. I am also grateful for Dr. Newmire for receiving the funding for this project.

Another professor I would like to thank is Dr. Gregory Buck for his support and continuous mentoring. Being a Teaching Assistant for the microbiology labs allowed me to explore my interest in academia.

I would like to thank the graduate and undergraduate students in our lab for supporting me along every step of the way. Both my fellow graduates, Janie Lindstrom and Lael Ceriani, were always there when I needed advice and help running my experiments. Working with them daily definitely made the journey more enjoyable.

This project was funded through the TCRF and RE Grants through the Texas A&M University-Corpus Christi.

TABLE OF CONTENTS

LIST OF FIGURES

FIGURES PAGE

LIST OF TABLES

TABLES PAGE

1. INTRODUCTION

1.1 DIABETES MELLITUS

Diabetes mellitus is a chronic metabolic disease affecting millions of people globally. It is classified as a heterogeneous disease where blood glucose levels are elevated above normal, a condition commonly known as hyperglycemia[1,2]. The American Diabetes Association diagnoses diabetes following a high blood sugar test, where the fasting plasma glucose is greater than or equal to 126 mg/dL, 2-hour post-meal plasma glucose levels greater than or equal to 200 mg/dL, or an HbA1C greater than or equal to 6.5% [3]. The HbA1c measures blood sugar concentrations over the past two months[3].

The disease is classified into three main groups, type 1 diabetes (T1D), type 2 diabetes (T2D), and gestational diabetes (GD). Type 1 diabetes is due to an autoimmune pancreatic β-cell destruction where the body does not produce insulin[4], while T2D is caused by a constant loss of β-cell insulin secretion[1], an impairment in insulin release and function. Gestational diabetes is a temporary condition occurring during pregnancy when the mother's blood glucose levels are higher than normal. While the exact mechanism of GD is still being studied, it is hypothesized placenta hormones block the action of the mother's insulin, resulting in insulin resistance[4]. Type 1 diabetes is congenital, while T2D is usually preventable with modification to diet, exercise, and close monitoring of blood glucose levels[2].

The most common form of diabetes is Type 2 Diabetes, accounting for 90-95% of all diabetes[1]. T2D is subject to various environmental and genetic factors leading to hyperglycemia and a decrease in β cell mass[1]. T2D does not utilize insulin properly, and over time the body is not able to produce enough insulin to maintain blood glucose levels[2]. The risk of developing T2D rises

with obesity, age, and lack of physical activity[1]. While GD is temporary, it increases the risks of both the mother and the offspring developing T2D[5].

Type 2 Diabetes is expected to affect approximately 8% of the world's population by 2030[6]. According to the National Diabetes Statistics Report 2020, published by the Centers for Disease Control and Prevention, in 2018, 34.2 million Americans have diabetes, where 7.3 million were undiagnosed. Of those diagnosed with diabetes, about 27% were individuals aged 65 years or older, and 210,000 children and adolescents younger than 20 years old were diagnosed with diabetes.

Among the adults diagnosed with diabetes, estimates for 2013-2016 indicated 21.6% of individuals were tobacco users, and 68.4% had a systolic blood pressure of 140 mmHg or higher, or diastolic blood pressure of 90 mmHg or higher; 89.0% were obese (BMI of 25 or higher) and 38.0% were physically inactive (defined as less than 10 minutes a week of moderate or vigorous activity). Fifty percent of the individuals had an A1C value of ≥ 7%, with a 43.5% non-HDL level of ≥ 130 mg/dL. Recent data indicate a higher rate of diabetes in American Indians, Alaskan Natives, Hispanics, and non-Hispanic blacks than in Asian Americans and non-Hispanic whites[7].

Skeletal muscle is the largest insulin-sensitive tissue in the body. Previous studies have shown low muscle mass and strength are associated with increased risk of T2D[8]. In older populations, T2D also appears to exacerbate the progression of sarcopenia or low muscle mass, which likely results in greater promotion of hyperglycemia. Additionally, age-related declines in muscle quality, including increased mitochondrial dysfunction and fat infiltration, are also implicated in skeletal muscle inflammation and subsequent insulin resistance[8].

1.2 SKELETAL MUSCLE

In mammals, skeletal muscles are composed of various muscle fibers with diverse properties and functions[9]. Skeletal muscle represents about 40-50% of total body mass and accounts for 80% of glucose uptake under euglycemic hyperinsulinemic conditions[8,10]. As the largest insulin-sensitive tissue[11], skeletal muscles play a vital role in healthy aging, and muscle mass loss is present in various diseases including sarcopenia, cancer cachexia, and bed rest, displaying the importance of growth and maintenance of muscle mass[10].

Based on the expression of myosin heavy chain (MHC) isoforms of the muscle fibers, different mammals have distinct expressions. Humans have three fiber types known as Type I slow-twitch, Type IIa fast-twitch, and Type IId/x fast-twitch with a glycolytic metabolic profILe[9]. Type I are slow force generators, mostly used for long-endurance movements, and have high mitochondria and capillary supply[9,12]. Type IIa are fast-twitch fibers and used in powerful bursts of movements, with similar oxidative profiles as Type I fibers. Type IId/x have low mitochondria and capillary supply, but high in glycolytic enzyme expression[9].

While some proteins produced by the muscle cells are released into circulation, others stay within the muscle, undergo an autocrine or paracrine mechanism, and express their signaling pathways within the muscle; this indicates some cytokines, also referred to as myokines, have the capability of mediating multiple health benefits and are facilitated during and post-exercise[13]. Lack of physical activity or muscle inactivity, in theory, leads to an altered myokine response, thus increasing the risk of various diseases including T2D[13].

A common overlooked occurrence in diabetic individuals is muscle myopathy, and it contributes to the progression of diabetic complications[14]. This helps outline the vital role of skeletal muscle in the prevention of disease. Additionally, since the skeletal muscle functions as

the largest site for glucose uptake, muscle myopathy can have adverse effects on the whole-body glucose homeostasis[15].

1.3 THERMOTHERAPY TREATMENT

Passive heat therapy is an immerging intervention to improve various health-related Illnesses, including cardiovascular health[16] and skeletal muscle metabolism. This viable alternative is potentially beneficial for patients with limited exercise capabilities and includes the elderly, obese, and diabetics. Humans show an adaptation to thermoregulation and capacity to work in hot environments when exposed to chronic exposure of heat[17].

There is a correlation between aging and insulin resistance in skeletal muscle, along with decreased insulin-stimulated glucose uptake[18]. In 1999, Hooper *et al.* analyzed the benefits of utilizing hot tubs for therapy as a means of mimicking the beneficial effects of exercise[19]. The experimental design was conducted on eight T2D patients, with water up to their shoulders. The experiment was performed for 30 minutes a day, six days a week, for three weeks, where the tub's water temperature was 40°C[19].

As the experiment progressed, the weight of the patients decreased, along with their mean fasting plasma glucose levels. The patients described an improved sleep cycle, and tests found a reduction in insulin dosage in one patient[19].

Skeletal muscles typically function above core temperature during exercise; thus, it is expected to have elevations in temperature. A 2016 study assessed the effect of chronic passive heat exposure on muscle contractility in humans. After exposure to 11 consecutive days of passive heat acclimation, skeletal muscle contractility increased in both hot and cool temperatures, along with maximal voluntary torque production. Such improvements following the repeated passive

exposure improve overall muscle function[20]. At rest, the human skeletal muscle is 2-4°C lower than the core temperature, while in endurance exercise, it can elevate up to 1°C above core temperature – reaching a temperature of 41°C in humans[21–23]

A 2020 study assessed the effect of chronic heat treatment on skeletal muscle function and structure in humans[24]. In the study, heated garments were applied to the thighs of the participants for 8 consecutive weeks. Following biopsies from vastus lateralis muscles, a temporal decline was present in capillarization around type II fibers, an elevation in endothelial nitric oxide synthase, and an increase in heat shock proteins HSPB5 and HSPB1[24]. Such findings support the use of the passive heat stress method as a therapeutic option for muscle weakness and capillary rarefaction.

1.4 CYTOKINE EXPRESSION AND INFLAMMATION

The skeletal muscles produce various cytokines in response to receptor-mediated signals along with disturbances to internal hemostasis, including cellular stress[21]. Feghali and Wright demonstrated acute inflammation is associated with the production of cytokines interleukin IL)-1, IL-6, and tumor necrosis factor -α (TNF-α); while chronic inflammation is involved in the production of cytokines IL-1, IL-4, IL-6, IL- 10, TNF-α[25].

The primary difference was the presence of IL-4 and IL-10 in chronic inflammation. In 2012, a research study demonstrated the cytokines IL-1β, IL-6, and TNF-α are strong promoters of inflammation while IL-4 and IL-10 are anti-inflammatory[26]. Specifically, IL-4 targets IL-1β to suppress inflammation, while IL-10 targets both IL-6 and TNF-α to block and regulate inflammation[26].

Tumor necrosis factor-α (TNF-α) serves as an inflammatory molecule and leads to the signaling of apoptosis and necrosis[27], while IL-10 is anti-inflammatory that targets and inhibits its

synthesis and activity of proinflammatory cytokines[28]; a recent study observed IL-10 signaling in skeletal muscle yielded a positive correlation with glucose metabolism in diabetic mice[28]. Interleukin-6 is secreted in abundance from skeletal muscles in response to hyperthermia, which supports skeletal muscles being an endocrine source for IL-6 during exercise[29].

Interleukin-6 is commonly classified as a pleiotropic cytokine because it plays a role in various biological functions including inflammation and immune responses, along with the development of nervous and hematopoietic systems[30]. Trans-signaling on IL-6 leads to pro-inflammatory properties, while the classic signaling pathway yields anti-inflammatory actions of this cytokine[31]. Dysregulation of IL-6 leads to chronic inflammation and autoimmunity, including rheumatoid arthritis[30].

Interleukin-10 plays an immunosuppressive role in the regulation of proinflammatory cytokines. This anti-inflammatory cytokine inhibits pro-inflammatory cytokines through suppressive effects on antigen-presenting cells and upregulation of anti-inhibitory genes[32]. IL-10 can inhibit the classical activation and enhance alternative activation of macrophages; the cytokine also inhibits interferon-gamma (IFN-γ), a crucial pro-inflammatory cytokine against pathogenic infections[32].

Interleukin-1β, a member of the IL-1 family, is a pro-inflammatory cytokine produced in response to infectious or inflammatory stimuli. IL-1 is known to play a role in innate immunity responses, along with a role in mediating fever and inducing several components of the acute-phase response[33]. In acute inflammation, the upregulation of IL-1β results in adaptive anti-tumor responses through an increased immunopathology of T helper 17 cells (Th17), along with differentiation of monocytes into dendritic cells; in chronic inflammation, however, upregulation of IL-1β increases the risk of cancer[33–35].

Interleukin-4 is a key cytokine for type II inflammatory response. IL-4 is known to induce the fusion of macrophages, and an upregulation leads to enhancing cell proliferation, survival, and differentiation[36]. This anti-inflammatory cytokine suppresses lipopolysaccharide-induced TNF-α at the level of transcription[37].

A recent study assessed the role of hyperthermia on skeletal muscle cells and affirmed physiological hyperthermia increases the mRNA responses to receptor-mediated IL-6 gene expression in skeletal muscles[21]. Previous studies showed an increase in the body's core temperature inhibited lipopolysaccharide-induced IL-6 secretion in inflammatory cells and fibroblasts[38]. In gastrointestinal enterocytes, hyperthermia amplifies IL-1β induced IL-6 [21].

1.5 PURPOSE

The purpose of this study was to assess the effect of acute and chronic heat treatment on gene expression and inflammatory markers in Type 2 Diabetic and healthy human skeletal muscle cells.

2. OBJECTIVES

Objective one assessed the effects of acute and chronic thermotherapy on HSMM and D-HSMM's cell viability and cell count.

Objective two assessed the thermotherapies' influence on gene expression in both skeletal muscle cell lines.

Objective three investigated the thermotherapies' impact on inflammation in the healthy and the diabetic human skeletal muscle cell lines, in particular, Interleukin – 1β, IL-4, IL-6, IL-10, and Tumor necrosis factor α (TNF-α).

3. RESEARCH DESIGN

3.1 SKELETAL MUSCLE CELL LINE DEMOGRAPHICS

Two skeletal muscle cell lines were purchased from Lonza Inc., Walkersville, MD – healthy human skeletal muscle myoblasts, and Type 2 Diabetes human skeletal muscle myoblasts, referred to as HSMM and D-HSMM, respectively. According to Lonza Inc., the cells were isolated from donated human tissue following informed and legal consent. The HSMM cell-line was acquired from a 38-year-old Caucasian male with a BMI of 26, while the D-HSMM cell line was acquired from a 68-year-old Caucasian male, shown in Table 1.

Table 1: Skeletal muscle Cell Line Characteristics

	HSMM	**D-HSMM**
Donor Age (years)	38	68
Donor Race	Caucasian	Caucasian
Donor Sex	Male	Male
Donor BMI	26	--
Virus Testing	Not detected	Not detected
Microbial Testing	Negative	Negative
Cell Performance: Viability	91%	93%

3.2 MEDIA PREPARATION

Skeletal Muscle Growth Media-2 (SKGM-2) was prepared by mixing contents of the SkGM-2 SingleQuots Kit (Lonza Inc.) into SkBM-2 Basal Medium (Lonza Inc.), followed by 5 mL of Penicillin-Streptomycin (1,000 units/mL) (Thermo Fisher Scientific) - referred to as SkMM.

The SkGM-2 SingleQuots Kit included 0.50 mL GA-1000, 0.50 mL hEGF, 0.50 mL Dexamethasone, 50.00 mL FBS, and 10.00 mL L-Glutamine. Filtration of the mixture was performed in a sterile environment inside a biosafety cabinet while being aliquoted into 50-mL centrifuge tubes. The tubes were stored at -20°C; the media was thawed and warmed to 37°C before usage.

3.3 SKELETAL MUSCLE CELL MAINTENANCE

3.3.1 INITIAL SEEDING

For the initial seeding of each cell line, 5 mL of SkMM was added into a 25 cm^2 culture vessel and incubated for 45 minutes at 37°C and 5% CO_2. Under a biosafety cabinet, the caps of the cryovials were briefly twisted to relieve pressure, and then retightened. Both HSMM and D-HSMM cryovials were placed in a 37°C water bath for a maximum of 2 minutes. In a biosafety cabinet, the cells were resuspended using a micropipette, and the cryovial content was transferred into the appropriate 25 cm^2 culture vessel. The vessels were rocked back and forth to evenly distribute the content, labeled, and stored in a 37°C and 5% CO_2 incubator (VWR, Radnor, PA). Upon reaching 70% confluency, the T-25 culture vessels were transferred into a T-75 culture vessel for increased surface area.

SkMM was changed every other day, or when the media's color began to change. In a sterile environment, the original media were aspirated from the culture vessel, and the same amount of fresh warmed media was added. The culture vessel was then stored in the 37°C and 5% CO_2 incubator.

3.3.2 SUB-CULTURING THE CULTURE VESSEL

Cell lines were passed when the vessel's confluency reached 70%. The growth medium was aspirated from the culture vessel, and the cells were rinsed with 5 mL of room temperature HEPES (4-(2-hydroxyethyl)-1-piperazineethanesulfonic acid) Buffer Saline Solution (HBSS) to neutralize the complex proteins in the growth medium that may inactivate trypsin. Two mL of trypsin was added to the vessel and incubated at 37°C for 6 minutes to allow the cells to detach from the culture vessel. Under a microscope, the vessels were checked to confirm detachment at the end of the 6 minutes. To neutralize the trypsin, 4 mL of Trypsin Neutralizing Solution (TNS) was then added to the 25 cm^2 vessel.

The detached cells-and-solution mixture was transferred to a sterile 15 mL centrifuge tube. The culture vessel was examined under a microscope to ensure a successful harvest with less than 5% remaining cells. The 15 mL centrifuge tube was centrifuged at $200 \times g$ for 5 minutes to pellet the cells. The supernatant was then aspirated from the centrifuge tube, where 2 mL of growth medium was added to the pellet before the centrifuge tube was vortexed and set for cell count.

One hundred µL of the 2 mL was used for cell counting, and the remaining mixture was transferred into a new sterile 75 cm^2 culture vessel with 13 mL of growth media and stored in the incubator at 37^0C and 5% CO_2.

3.3.3 SKELETAL MUSCLE CELL COUNT AND VIABILITY

Cell counting was determined using a hemacytometer. In a sterile 0.5 mL Eppendorf tube, 100 µL of 0.4% Trypan Blue (Thermo Fisher Scientific) was mixed with 100 µL of cells from the 2 mL mix in the 15 mL centrifuge tube. The microcentrifuge tube was vortexed to ensure even distribution, and 10 µL of the mixture was loaded into the hemacytometer underneath the

coverslip. Using a microscope with a 10X objective, and a tally counter the live, unstained, cells were counted, shown in Figure 1. The dead, stained, cells were also documented. The four large corner grids and the large middle grid were counted[39].

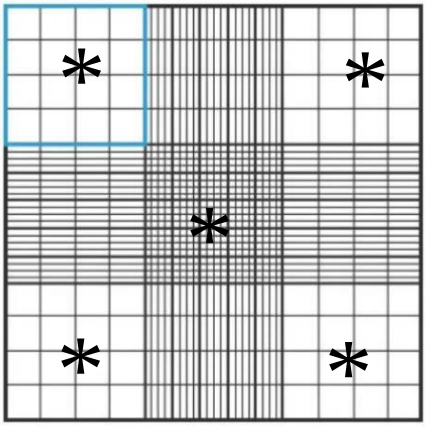

Figure 1: Hemacytometer gridlines indicating one of the sets of 16 squares. The asterisk (*) represents the grids that were counted.

Cell viability was calculated by $\frac{live\ cell\ count}{total\ cell\ count} \times 100$. Total cell count was determined by adding the live cells total and the dead cells total. To determine density, *cells/ µL*, the following equation was used: $\frac{viable\ cell\ count}{5} \times 10^4 \times 2$, where 5 represents the number of large grids counted, 10^4 is the conversion factor from µL to mL, and 2 represents the dilution factor of Trypan Blue[39]. With both chambers of the hemacytometer charged, the total cell viability and count were determined by averaging the data of both chambers.

3.4 THERMOTHERAPY TREATMENTS

3.4.1 PLATE SET-UP

Acute and chronic heat treatments were applied to both cell lines. The acute thermotherapy was a one-time exposure to 40°C for 30 minutes. The chronic thermotherapy constituted a 30-minute exposure to 40°C, three times a week, for three weeks.

Each cell line was inoculated into 4 wells of a 24-well plate, as shown in Figure 2. Upon transferring from a T-75 mL culture vessel, cell count and viability were determined. Per well, 10^5 cells were seeded along with growth media, totaling a volume of 2 mL. Additionally, 2 mL of growth media were added into the 4 wells of the plate as a control. The 24-well plate was then stored at 37°C and 5% CO_2 for 48 hours. Three 24-well plates were prepared for acute, chronic, and control.

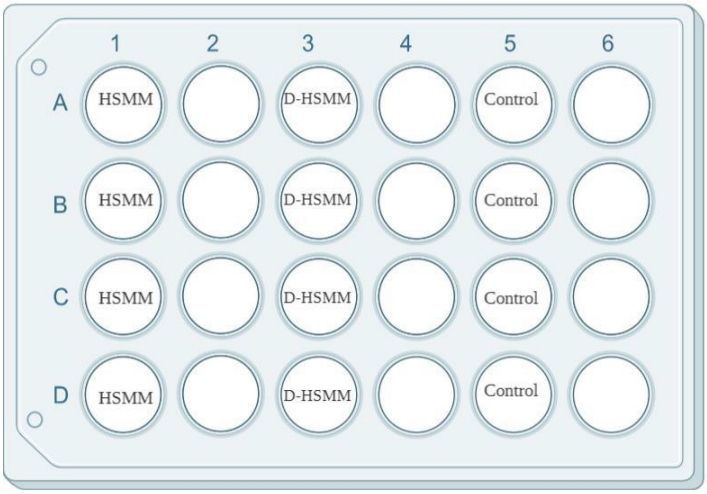

Figure 2: Overview of the plate layout.

3.4.2 CHRONIC THERMOTHERAPY

Following the 48-hour incubation session, the chronic plate was placed at 40°C and 5% CO_2 for 30 minutes, then stored at 37°C and 5% CO_2. Wells were observed for morphology and confluency before and after each treatment. The plate was placed at 40°C and 5% CO_2 three times a week for three weeks, as outlined in Table 2. The plate was subjected to the temperature increase three days a week for 30 minutes over an 18-day span.

3.4.3 ACUTE THERMOTHERAPY

Following the 48-hour incubation session, the plate was placed at 40°C and 5% CO_2 for 30 minutes. Before and after the heat exposure, wells were observed for morphology and confluency. The plate was subjected to 40°C and 5% CO_2 on the scheduled day outlined in Table 2.

3.4.4 CONTROL PLATE

To serve as a control, no heat treatment, a third plate was seeded and incubated at 37°C and 5% CO_2 for the duration of the 3-week thermotherapy treatment.

Table 2: Schematic overview of the thermotherapy protocol.

Week	Day Number	Day	Date	Time	Description
0	0	Saturday	3/30/2019	11 am	Seeded for chronic and control
1	1	Monday	4/1/2019	10 am – 10:30 am	Chronic treatment
	2	Wednesday	4/3/2019	10 am – 10:30 am	
	3	Friday	4/5/2019	10 am – 10:30 am	
2	1	Monday	4/8/2019	10 am – 10:30 am	
	2	Wednesday	4/10/2019	10 am – 10:30 am	
	3	Friday	4/12/2019	10 am – 10:30 am	
3	1	Monday	4/15/2019	10 am – 10:30 am	
	2	Wednesday	4/17/2019	10 am – 10:30 am	- Chronic treatment - Seeded for Acute
	3	Friday	4/19/2019	10 am – 10:30 am	Chronic and Acute treatments

3.5 CELL COUNT AND VIABILITY

To assess Objective 1, the total cell count was calculated 24 hours after each treatment. The media in each well of the three experimental plates was aspirated, and 2 mL of HBSS was used to rinse each well. Following the rinse, 0.8 mL of Trypsin was added to the wells and the plate was incubated at 37°C for 6 minutes. Under a microscope, the plates were checked to confirm detachment at the end of the 6 minutes, and 1.0 mL of TNS was then added to each well.

The detached cells-and-solution mixture was transferred to a sterile 2 mL microcentrifuge tube. The experimental plate was examined under a microscope to ensure a successful harvest with less than 5% remaining cells. The microcentrifuge tube was centrifuged at $200 \times$ g for 5 minutes to pellet the cells.

The supernatant was then aspirated from the centrifuge tube, 2 mL of growth medium were added, and the tube was vortexed and set for cell count. One hundred µL of the 2 mL was used for cell counting based on the protocol described in *Section 3.3.3 Cell Count and Viability*. Each well was tallied twice, and the numbers were averaged to determine the cell count. The remaining 1.9 mL was centrifuged at $200 \times$ g for 5 minutes and mixed with 0.25 mL of fresh new media in preparation for RNA purification.

3.6 RNA PURIFICATION

To isolate high-quality RNA from the samples, Invitrogen TRIzol Reagent (Thermo Fisher Scientific) was used. To the 0.25 mL mixture prepared, 0.75 mL of TRIzol was added. The mixture was homogenized and incubated for 5 minutes to allow for dissociation of the nucleoproteins complex. To the mixture, 150 µL of chloroform was added and incubated for 3 minutes. The tube was centrifuged for 15 minutes at $12{,}000 \times$ g at 4°C. The aqueous solution was transferred to a new tube.

The RNA was precipitated by adding 375 µL of isopropanol, then incubated for 10 minutes. The mixture was centrifuged for 10 minutes at $12{,}000 \times$ g at 4°C. The supernatant was discarded and 750 µL of 75% ethanol was added. The tube was briefly vortexed and centrifuged for 5 minutes at $7{,}500 \times$ g at 4°C. The supernatant was removed, and the pellet was airdried for 8 minutes. The RNA was solubilized by being resuspended in 50 µL of RNAase-free water. RNA purity and concentration were then quantified using a 1-position Spectrophotometer (Thermo Fisher Scientific). The samples were stored at -80°C.

3.7 GENE EXPRESSION

Objective 2 was assessed by performing a real-time polymerase chain reaction (RT-PCR) to qualitatively assess which genes were regulated in each experimental condition. The purified RNA was converted to C_T using the TaqMan RNA-to-C_T 1-Step Kit (Thermo Fisher Scientific). For a total volume of 20 µL per one reaction, 10.0 µL of TaqMan RT-PCR Mix (2X) was mixed with 0.5 µL of TaqMan RT Enzyme Mix (40X), and 9.5 µL of RNA template + RNase-free water. The RNA template recommended was 50 ng per well. The total volume of RNA varied based on the purified concentration of each sample and is shown in Table 3.

Table 3: Total RNA Volume Used for PCR. The amount was based on the purified concentration of each sample.

Sample	Amount of RNA used per reaction
Acute Diabetic	0.82 µL
Acute Healthy	2.55 µL
Chronic Diabetic	0.02 µL
Chronic Healthy	0.02 µL
Control Diabetic	0.02 µL
Control Healthy	0.04 µL

A Custom TaqMan Array 96-well plate (4391524) was formatted with targeted genes found in human skeletal muscles; the assessed genes are shown in Table 5. One plate was used for each sample described in Table 3. Each well of the 96 custom plate was loaded with 20 µL of the sample, and a QuantStudio 3 Real-Time PCR Instrument (Thermo Fisher Scientific) was programmed based on manufacturer's protocol outlined in Table 4. The experiment was performed, and the results were analyzed on Thermo Fisher Cloud using Eukaryotic 18S ribosomal RNA as the endogenous gene and the reference sample being the control of each cell type. The complete 96 assessed genes are shown in Table 5.

Table 4: PCR Cycling Conditions per manufacturer's protocols.

Stage	Step	Temp	Time
Holding	Reverse transcription	48°C	15 minutes
Holding	Activation of AmliTaq Gold Polymerase	95°C	10 minutes
Cycling (40 cycles)	Denature	95°C	15 seconds
	Anneal/Extend	60°C	1 minute

Table 5: Ninety-six biomarkers assessed through real-time PCR.

Eukaryotic 18S rRNA	Dystroglycan 1	Lamin A/C	PPARG Coactivator 1 A
Actin	Desmin	Mitogen-Activated Protein Kinase 14	PPARG Coactivator 1 B
Actin B	Dystrophin	Mitogen-Activated Protein Kinase 1	Peroxisome Proliferator-Activated Receptor Gamma
Actinin A 3	Dystrophia Myotonica Protein Kinase	Mitogen-Activated Protein Kinase 3	Protein Phosphatase 3 Catalytic Subunit A
Activin A Receptor Type 2B	Dysferlin	Mitogen-Activated Protein Kinase 8	Protein Kinase Amp-Activated catalytic subunit A1
Adiponectin	F-Box Protein 32	Myoglobin	Protein Kinase Amp-Activated Non-Catalytic Subunit B 2
Adrenoceptor B 2	Fibroblast Growth Factor 2	Myocyte Enhancer Factor 2C	Protein Kinase Amp-Activated Non-Catalytic Subunit Gamma 1
Agrin	Forkhead Box O1	Matrix Metallopeptidase 9	Protein Kinase Amp-Activated

			Non-Catalytic Subunit Gamma 3
AKT Serine/Threonine Kinase-1	Forkhead Box O3	Myostatin	Ras Homolog Family Member A
AKT Serine/Threonine Kinase-2	Glyceraldehyde-3-Phosphate Dehydrogenase	Muscle Associated Receptor Tyrosine Kinase	Ribosomal Protein Lateral Stalk Subunit P0
ATPase Sarcoplasmic/Endoplasmic Reticulum Ca2+ Transporting 1	Glucuronidase B	Myogenic Factor 5	Ribosomal Protein S6 Kinase B1
B-2-Microglobulin	Histone Deacetylase 5	Myogenic Factor 6	Sarcoglycan A
Bcl2	Hexokinase 2	Myosin Heavy Chain 1	Solute Carrier Family 2 Member 4
Bone Morphogenetic Protein 4	Hydroxymethylbilane Synthase	Myosin Heavy Chain 2	Tata-Box Binding Protein
Calcium/Calmodulin Dependent Protein Kinase Ii Gamma	Hypoxanthine Phosphoribosyltransferase 1	Myogenic Differentiation 1	Transferrin Receptor
Calpain 2	Insulin-Like Growth Factor 1	Myogenin (Myogenic Factor 4)	Transforming Growth Factor B 1
Calpain 3	Insulin-Like Growth Factor 2	Myotilin	Tumor Necrosis Factor
Caspase 3	Insulin-Like Growth Factor-Binding Protein 3	Nebulin	Troponin C1
Calpastatin	Insulin-Like Growth Factor-Binding Protein 5	Nuclear Factor Kappa B Subunit 1	Troponin I2
Caveolin 1	Inhibitor of Kappa Light Polypeptide Gene Enhancer In B-Cells	Nitric Oxide Synthase 2	Troponin T1
Caveolin 3	Interleukin 1 B	Paired Box 3	Troponin T3
Crystallin A B	Interleukin 6	Paired Box 7	Tripartite Motif-Containing 63
Citrate Synthase	Importin 8	Pyruvate Dehydrogenase Kinase 4	Titin
Catenin B 1	Leptin	Phosphoglycerate Kinase 1	Utrophin

3.8 ENZYME-LINKED IMMUNOSORBENT ASSAY

Enzyme-linked immunosorbent assays (ELISA) were utilized for the quantification of inflammatory antigens in the cell supernatant. The assessed markers include human Interleukin (IL) -1β, IL-4, IL-6, IL-10, and Tumor necrosis factor α (TNF-α). All ELISA kits were obtained from Thermo Fisher Scientific, and all reagents were at room temperature before using. For each of the markers, we followed the suggested manufacturer's protocol.

3.8.1 INTERLEUKIN – 1β

Per the manufacturer's protocol (BMS224-2), standards were prepared based on a 1:2 serial dilution with a concentration range from 250.0 pg/mL to 3.9 pg/mL. The microstrips were washed twice with 400 µL of Wash Buffer per well with thorough aspiration in between washes. One hundred µL of each standard dilution created was added in duplicate, while 100 µL of Sample Diluent was added in duplicate to the blank wells. Fifty µL of Sample Diluent was added to each sample well, followed by 50 µL of each sample. Fifty µL of Biotin-Conjugate was added to all the wells, and adhesive film covered the microstrips as they incubated at room temperature for 2 hours.

Following the incubation, the wells were washed 3 times with Wash Buffer, then 100 µL of diluted Streptavidin-HRP was added to all the wells of the microstrip. The wells were then covered with an adhesive film and incubated at room temperature for 1 hour. At the end of the hour, the microwell strips were washed 3 times with Wash Buffer. One hundred µL of TMB Substrate Solution was added to all the wells and incubated at room temperature for 10 minutes in the dark. Following the dark incubation, 100 µL of Stop Solution was added to each well, and the absorbance of each well was quantified on a spectrophotometer (BioRad Laboratories, Hercules, CA) using 450 nm as the primary wavelength. The absorbance of both samples and standards was calculated.

A standard curve was created using the mean of the standards, and the concentration (pg/mL) of the samples was calculated.

3.8.2 INTERLEUKIN-4

Per the manufacturer's protocol (BMS225-2), standards were prepared based on a 1:2 serial dilution with a concentration range from 500.0 pg/mL to 7.8 pg/mL. The microstrips were washed twice with 400 µL of Wash Buffer per well with thorough aspiration in between washes. One hundred µL of each standard dilution created was added in duplicate, while 100 µL of Assay Buffer (1x) was added in duplicate to the blank wells. Fifty µL of Assay Buffer (1x) was added to each sample well, followed by 50 µL of each sample. Fifty µL of Biotin-Conjugate was added to all the wells, and adhesive film covered the microstrips as they incubated at room temperature for 2 hours.

Following the incubation, the wells were washed 3 times with Wash Buffer, then 100 µL of diluted Streptavidin-HRP was added to all the wells of the microstrip. The wells were then covered with an adhesive film and incubated at room temperature for 1 hour. At the end of the hour, the microwell strips were washed 3 times with Wash Buffer. One hundred µL of TMB Substrate Solution was added to all the wells and incubated at room temperature for 10 minutes in the dark. Following the dark incubation, 100 µL of Stop Solution was added to each well, and the absorbance of each well was quantified on a spectrophotometer (BioRad Laboratories, Hercules, CA) using 450 nm as the primary wavelength. The absorbance of both samples and standards was calculated.

A standard curve was created using the mean of the standards, and the concentration (pg/mL) of the samples was calculated.

3.8.3 INTERLEUKIN-6

Per manufacturer's protocol (EH2IL6), standards were prepared based on a 1:2.5 serial dilution, per manufacturer's protocol, with a concentration range from 400.0 pg/mL to 10.24 pg/mL and 0 pg/mL. Fifty µL of Biotinylated Antibody Reagent was added to each well. Fifty µL of the standards and samples were added in duplicate to the microstrip plate. This was followed by covering the plate with an adhesive film and incubating it at room temperature for 2 hours.

Following the incubation, the wells were washed by filling each well with 400 µL of Wash Buffer 3 times, then 100 µL of diluted Streptavidin-HRP was added to all the wells of the microstrip. The wells were then covered with an adhesive film and incubated at room temperature for 30 minutes. At the end of the incubation, the microwell strips were washed 3 times based on the protocol mentioned earlier. One hundred µL of TMB Substrate Solution was added to all the wells and incubated at room temperature for 30 minutes in the dark. Following the dark incubation, 100 µL of Stop Solution was added to each well, and the absorbance of each well was quantified on a spectrophotometer (BioRad Laboratories, Hercules, CA) using 450 nm as the primary wavelength. The absorbance of both samples and standards was calculated.

A standard curve was created using the mean of the standards, and the concentration (pg/mL) of the samples was calculated.

3.8.4 INTERLEUKIN-10

Per the manufacturer's protocol (BMS215-2), standards were prepared based on a 1:2 serial dilution with a concentration range from 200.0 pg/mL to 3.1 pg/mL. The microstrips were washed twice with 400 µL of Wash Buffer per well with thorough aspiration in between washes. One hundred µL of each standard dilution created was added in duplicate, while 100 µL

of Assay Buffer (1x) was added in duplicate to the blank wells. Fifty µL of Assay Buffer (1x) was added to each sample well, followed by 50 µL of each sample. Fifty µL of Biotin-Conjugate was added to all the wells, and adhesive film covered the microstrips as they incubated at room temperature for 2 hours.

Following the incubation, the wells were washed 3 times with Wash Buffer, then 100 µL of diluted Streptavidin-HRP was added to all the wells of the microstrip. The wells were then covered with an adhesive film and incubated at room temperature for 1 hour. At the end of the hour, the microwell strips were washed 3 times with Wash Buffer. One hundred µL of TMB Substrate Solution was added to all the wells and incubated at room temperature for 10 minutes in the dark. Following the dark incubation, 100 µL of Stop Solution was added to each well, and the absorbance of each well was quantified on a spectrophotometer (BioRad Laboratories, Hercules, CA) using 450 nm as the primary wavelength. The absorbance of both samples and standards was calculated.

A standard curve was created using the mean of the standards, and the concentration (pg/mL) of the samples was calculated.

3.8.5 TUMOR NECROSIS FACTOR – α

Per the manufacturer's protocol (BMS223-4), standards were prepared based on a 1:2 serial dilution with a concentration range from 500.0 pg/mL to 7.8 pg/mL. The microstrips were washed twice with 400 µL of Wash Buffer per well with thorough aspiration in between washes. One hundred µL of each standard dilution created was added in duplicate, while 100 µL of Sample Diluent was added in duplicate to the blank wells. Fifty µL of Sample Diluent was added to each sample well, followed by 50 µL of each sample. Fifty µL of Biotin-Conjugate was

added to all the wells, and adhesive film covered the microstrips as they incubated at room temperature for 2 hours.

Following the incubation, the wells were washed based on the protocol mentioned earlier 3 times, then 100 µL of diluted Streptavidin-HRP was added to all the wells of the microstrip. The wells were then covered with an adhesive film and incubated at room temperature for 1 hour. At the end of the hour, the microwell strips were washed 3 times with Wash Buffer. One hundred µL of TMB Substrate Solution was added to all the wells and incubated at room temperature for 10 minutes in the dark. Following the dark incubation, 100 µL of Stop Solution was added to each well, and the absorbance of each well was quantified on a spectrophotometer (BioRad Laboratories, Hercules, CA) using 450 nm as the primary wavelength. The absorbance of both samples and standards was calculated.

A standard curve was created using the mean of the standards, and the concentration (pg/mL) of the samples was calculated.

3.9 STATISTICAL ANALYSIS

Data collection during the heat treatment was done in quadruplicate, and each sample was analyzed twice with the mean recorded (*n=8)*. Data collected for gene expression was qualitative, while the data collected for inflammation was done in duplicate. Gene expression data are expressed as fold change, a multiplier of up or down-regulation compared to the control samples. To analyze data, GraphPad Prism version 8.0.0 (San Diego, California USA) was utilized. Cytokine concentrations were determined using a 5-parameter curve fit, per manufacturer protocols. A 2×2 analysis of variance (ANOVA) was used, along with a post hoc Tukey's Multiple Comparisons Test at a significance level of $\alpha < 0.05$ to test for significance among the means (n=8). Two 2×2 ANOVA assessments were performed: (1) within-subject factors –

analyzing pre-treatment and post-treatment concentrations; and (2) between-subject factors – comparing the treatment concentrations to the controls. The data were presented as a mean ± standard error of the mean (Mean ± SEM).

4. RESULTS

4.1 SKELETAL MUSCLE CELL VIABILITY

Figure 3 and Table 6 shows the change in cell viability of the human skeletal muscle myoblasts following each treatment. Overall, the chronic exposure to an environmental temperature of 40°C yielded a slight increase in cell viability. The acute treatment, however, caused a significant decrease in the D-HSMM sample ($p = 0.0006$), while the acute exposure on HSMM had no significant change in cell viability percentage.

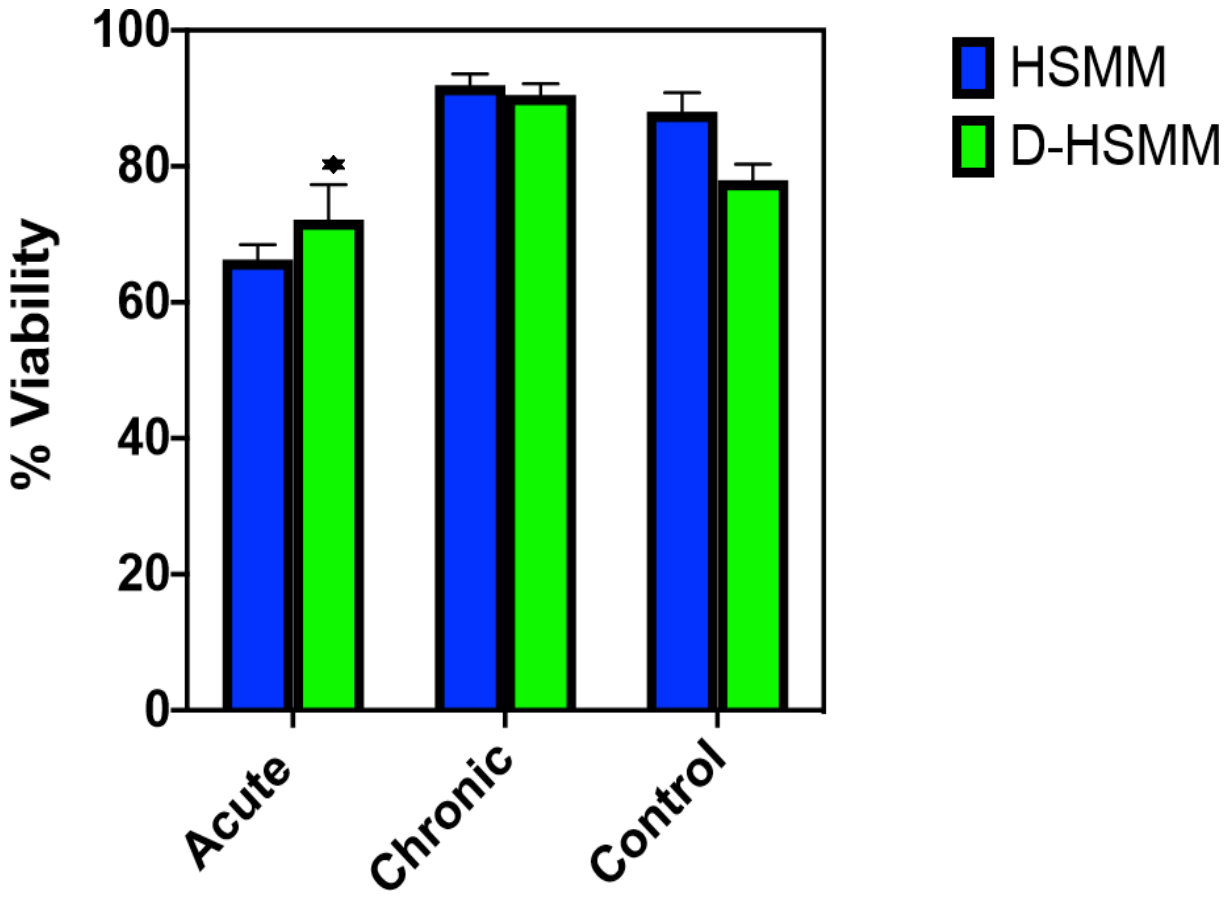

Figure 3: Following the acute and the chronic heat treatments, cell viability percentage increased following the chronic treatment, but decreased following the acute heat treatment. A significant decrease was noted in D-HSMM following the acute exposure ($p = 0.0089$). The asterisks (*) represent significance ($p<0.05$).

Table 6 shows the mean of each experimental group ± the standard error mean, and the results are expressed in percentage (%) form. In the control plate, HSMM had a mean cell viability percentage of 88.015%, while the D-HSMM resulted in mean cell viability of 77.953%. Quantitively, the chronic heat exposure to HSMM resulted in an approximate 1.04-fold increase, however, acute exposure to HSMM resulted in an approximate 1.33-fold decrease. A chronic exposure on D-HSMM yielded a 1.16-fold increase, while the acute treatment yielded a 1.08-fold decrease.

Table 6: Following the acute heat treatment, cell viability percentage of HSMM decreased by 1.33-fold, and by 1.08-fold in D-HSMM. The chronic heat exposure increased cell viability percentage by 1.04-fold in HSMM and 1.16-fold in D-HSMM. Data is shown in percentage form and presented in mean ± SEM.

	HSMM	**D-HSMM**
Acute	66.3 ± 2.174	72.150 ± 5.140*
Chronic	91.938 ± 1.647	90.515 ± 1.631
Control	88.015 ± 2.806	77.953 ± 2.354

4.2 GENE EXPRESSION

Figures 4 and 5 represent the top five genes expressed, regardless of treatment type, in HSMM and D-HSMM, respectively. Figure 6 Illustrates the expression of all genes assessed in HSMM and D-HSMM to the heat treatments. Each cell type had a control plate serving as the reference plate while *eukaryotic 18S rRNA* served as the endogenous gene. Of both cell lines, HSMM yielded a higher value of fold change than D-HSMM.

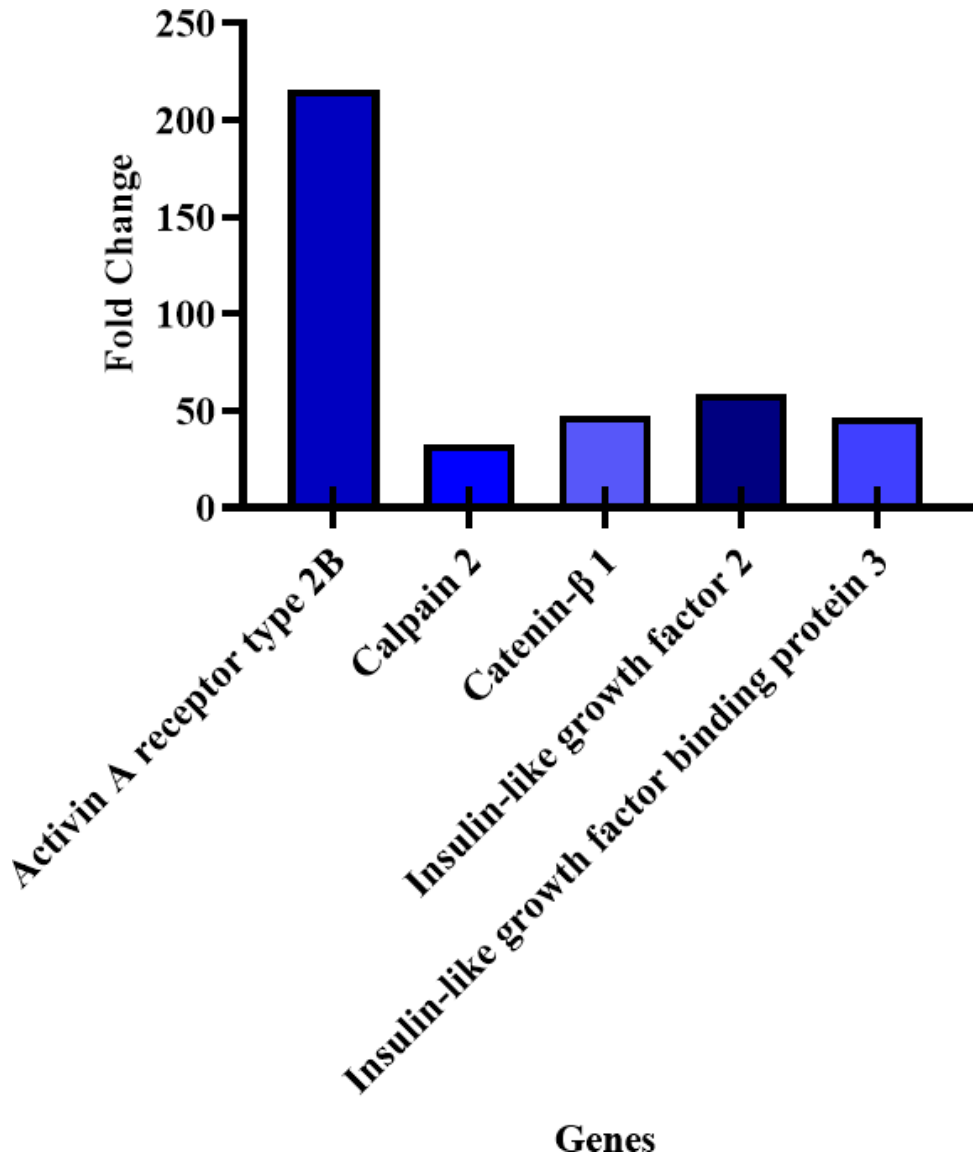

Figure 4: The top 5 genes expressed in HSMM following both acute and chronic treatments. All 5 genes expressed the highest fold-change occurred following the acute treatment. The up-regulated five genes had a range of 215.613 to 32.744-fold.

Figure 4 represents the five genes with the highest fold change in the healthy human skeletal muscle myoblasts; the top five upregulated genes were from the acute treatment. The range was 0.099 – 215.613-fold. Activin A receptor type 2B was upregulated 215.613-fold, followed by insulin-like growth factor 2 (59.063-fold), catenin-β 1 (47.492-fold), insulin-like growth factor binding protein 3 (46.719-fold), and calpain 2 (32.744-fold).

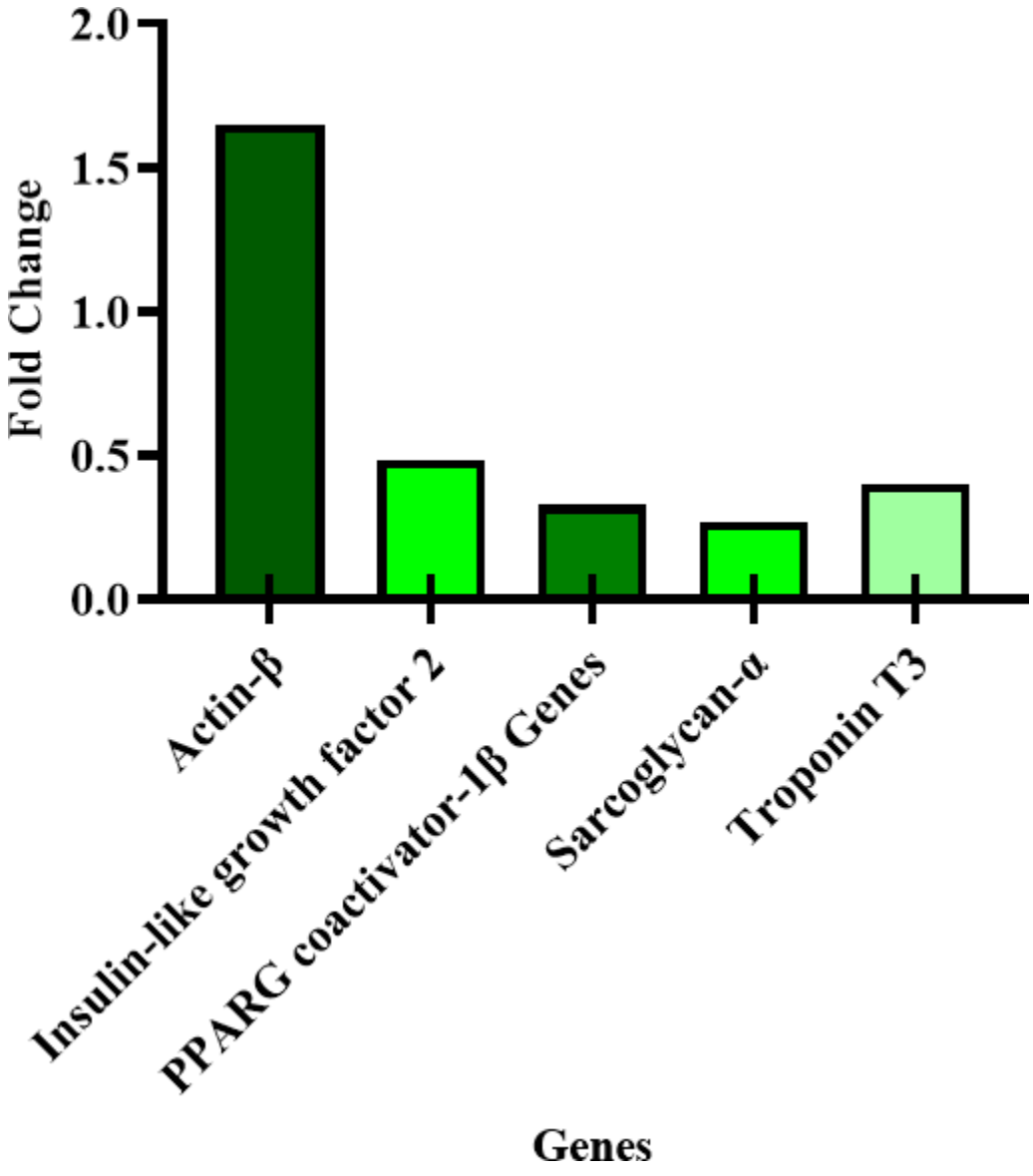

Figure 5: The top 5 genes expressed in D-HSMM following both acute and chronic heat treatments. Actin-β had the highest fold-change following the acute treatment, while the remaining top 4 genes occurred following the chronic treatment. The upregulation of these 5 genes had a range of 0.267 to 1.648-fold.

Figure 5 represents the five genes with the highest fold change in diabetic human skeletal muscle myoblasts. Excluding actin-β, the remaining four genes were upregulated in the chronic

treatment; actin-β was upregulated in the acute treatment. The range of upregulated D-HSMM genes was 0.001 – 1.648, with a mean of 0.073. Actin-β was upregulated by 1.648-fold, followed by insulin-like growth factor-2 (0.485-fold), troponin T3 (0.399-fold), PCG coactivator-1β (0.328-fold), and sarcoglycan-α (0.267-fold).

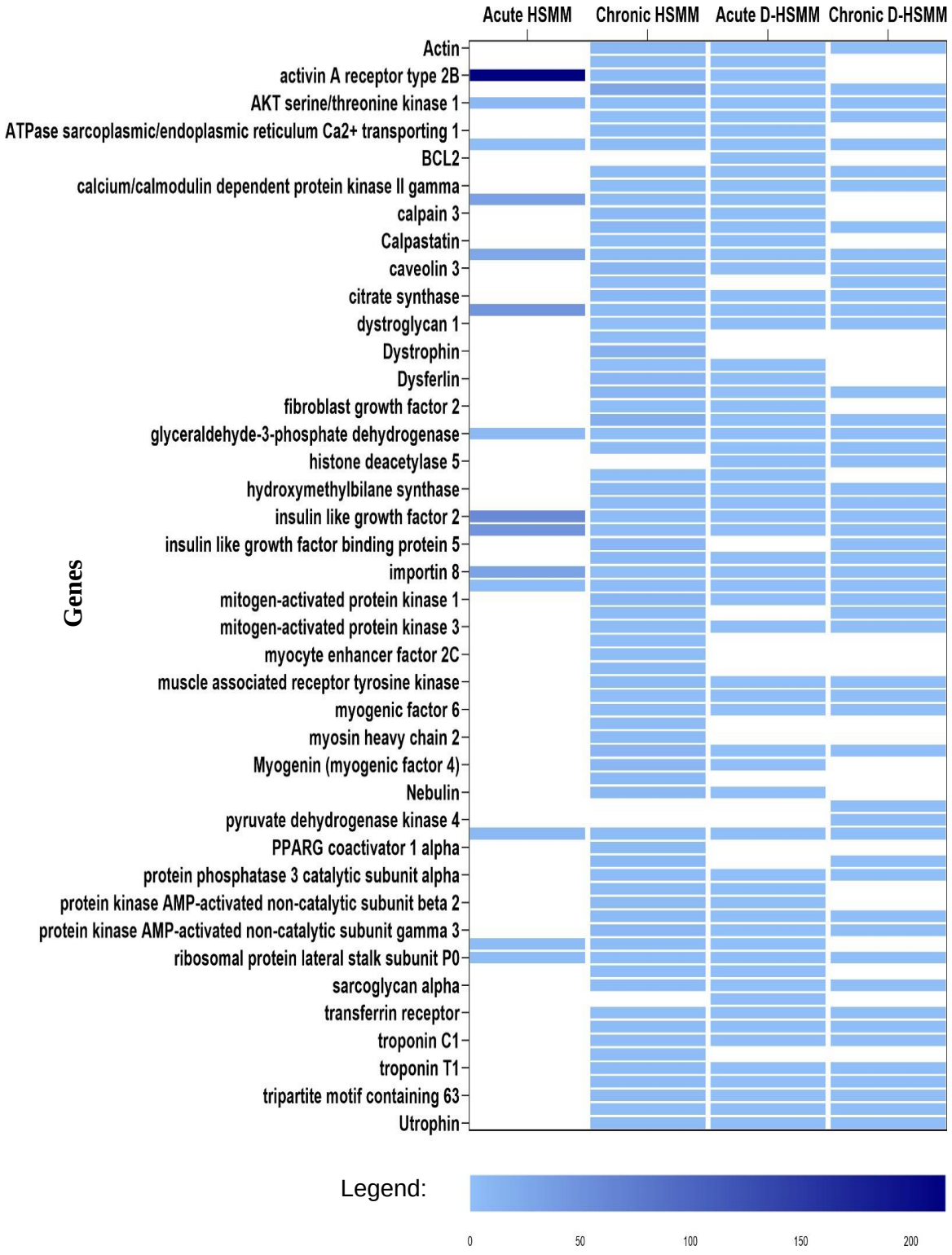

Figure 6:Gene expression of qualitatively assessed genes in HSMM and D-HSMM following the acute and chronic heat treatments. All values are expressed in fold-change compared to the control, with eukaryotic 18S rRNA as the endogenous control.

Figure 6 lists the overexpressed genes in HSMM and D-HSMM following the acute and chronic treatments. This qualitative assessment shows the fold change as compared to the control. A change in expression was more evident in HSMM following the chronic exposure, while in D-HSMM, the chronic exposure yielded minimal changes in expression.

HSMM, exposed to the acute treatment, had a range of 1.193 – 215.613, while the chronic treatment had a range of 0.099 – 26.714. The D-HSMM exposed to the acute treatment had a range of 0.001 – 1.648, while the chronic treatment yielded a range of 0.012 – 0.485. In total, 14 genes were expressed in HSMM following the acute treatment, while 74 genes were expressed following the chronic treatment. In D-HSMM, 40 genes were expressed following the acute treatment, while 51 were expressed following the chronic treatment.

4.3 INFLAMMATORY MARKERS

To determine whether the thermotherapies resulted in cytokine production, cytokines IL-1β, IL-4, IL-6, IL-10, and TNF-α were assessed by ELISA. The soluble cytokines were measured from culture supernatant following a 24-hour incubation post-treatment.

4.3.1 INTERLEUKIN 1β

Figure 7 represents the concentration of cytokine IL-1β following both the acute and the chronic treatments on HSMM and D-HSMM. A significant correlation was evident between the two cell types ($p = 0.0092$) when comparing the cytokine expression before and after each treatment. Additionally, the treatments yielded a significant change of IL-1β concentration ($p = 0.0009$), compared to the controls. Following the acute treatment, a significant decrease was seen in HSMM ($p = 0.0036$) and D-HSMM ($p = 0.0461$), compared to the controls. Following the chronic treatment, HSMM ($p = 0.0133$) also had a significant decrease, however, change in D-HSMM ($p = 0.1836$) was not significant, compared to the control.

Table 8 presents the average of IL-1β concentrations following the treatments. In both HSMM and D-HSMM, the concentrations following the acute and the chronic treatments were less than the control. In HSMM, the acute treatment yielded a 50.43-fold decrease, while the chronic treatment yielded a 2.61-fold decrease. In D-HSMM, the acute treatment resulted in a 1.85-fold decrease while the chronic treatment had a 1.73-fold decrease.

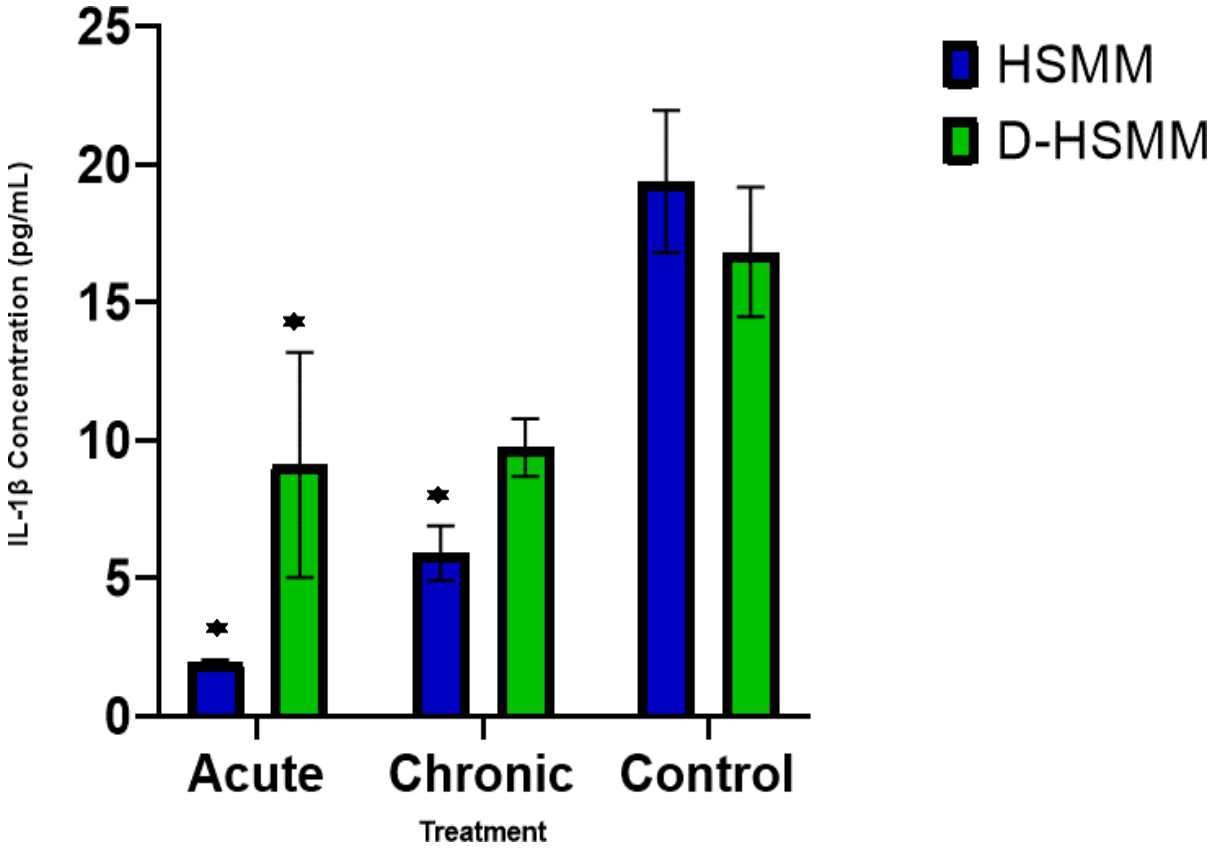

Figure 7:Following both heat treatments (p = 0.0009), the concentration of IL-1β significantly decreased, except in D-HSMM following the chronic treatment. The significant decrease was evident following the acute treatment on HSMM (p = 0.0036), D-HSMM (p = 0.0461), and following the chronic treatment on HSMM (p = 0.0133). Concentration is presented in pg/ mL ± SEM.

Table 7: The concentration average of IL-1β in HSMM and D-HSMM following the heat treatments. A significant decrease is evident following the acute and chronic heat treatments on the cytokine expression in HSMM. This significant decrease is also evident in D-HSMM following the acute treatment. The data is represented in mean ± SEM, in pg/mL. The asterisk (*) indicates a significant change.

	HSMM (pg/mL)	**D-HSMM (pg/mL)**
Acute	1.988 ± 0.051 *	9.110 ± 2.882 *
Chronic	5.916 ± 0.984 *	9.740 ± 0.735
Control	19.373 ± 2.572	16.820 ± 1.661

4.3.2 INTERLEUKIN-4

Figure 8 Illustrates the cytokine concentration in HSMM and D-HSMM following acute and chronic heat treatments. A statistical significance was evident in the treatments ($p = 0.0043$). A significant decrease was evident following the chronic treatment on D-HSMM ($p = 0.0176$). No significant change was noted following the acute treatment, nor in the HSMM cell type. Assessing within-subject factors (pre-treatment and post-treatment) the cell type yielded a significant change compared to each other ($p = 0.0019$).

Table 9 outlines the concentration of IL-4 following the acute and the chronic treatments on HSMM and D-HSMM. A decrease is apparent following both treatments compared to the control. IL-4 expression in HSMM decreased by 1.90-fold following the acute treatment, and by 3.38-fold following the chronic treatment. The cytokine expression in D-HSMM decreased by 2.28-fold following the acute treatment and 18.81-fold following the chronic treatment.

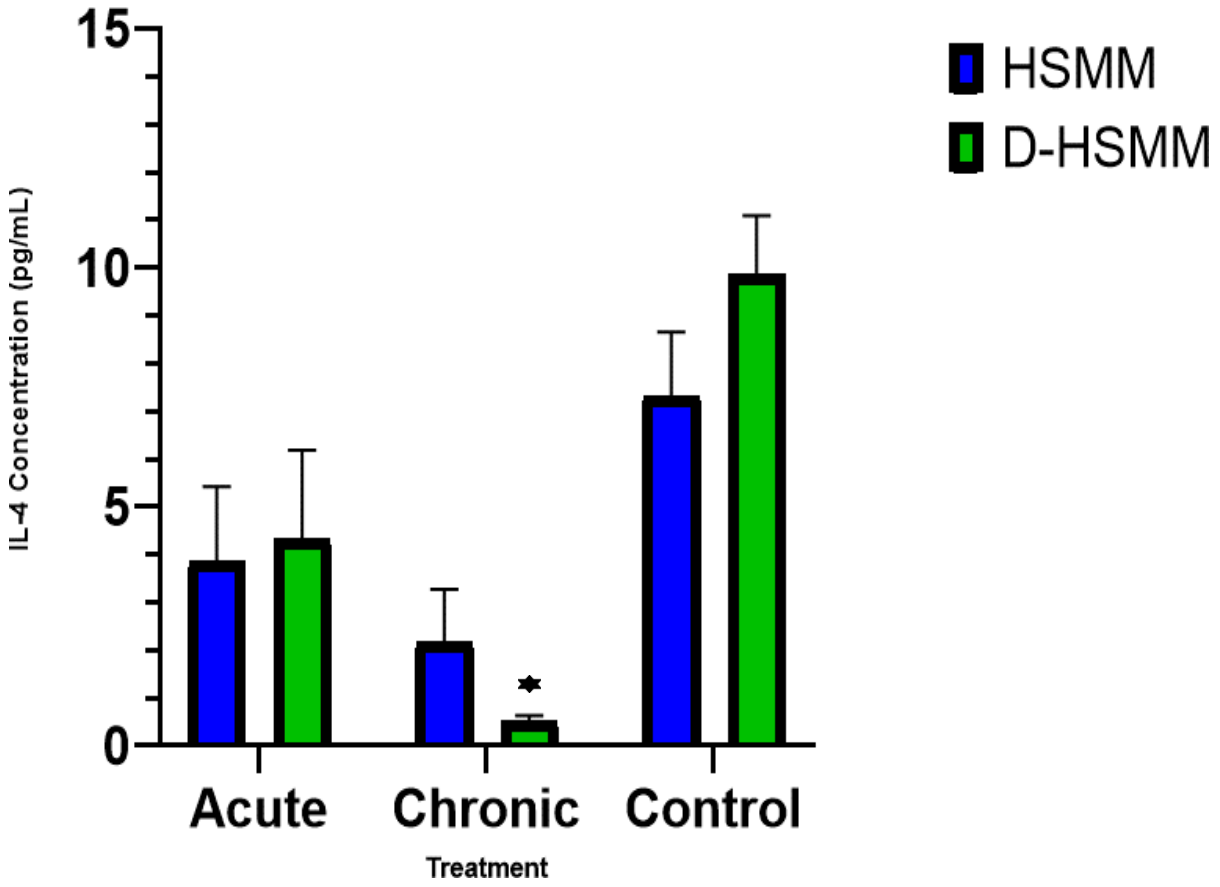

Figure 8: Following the heat treatments (p = 0.0043), the concentration of IL-4 decreased in both HSMM and D-HSMM cell lines. A significant decrease was evident in D-HSMM (p = 0.0176) following the chronic treatment. Cytokine concentration was measured in pg/mL, and data were recorded as mean ± SEM. The asterisk (*) indicates a significant change

Table 8: The average concentration of IL-4 following the acute and chronic treatments in HSMM and D-HSMM cell lines (p = 0.0019). A decrease in cytokine concentration is evident in both HSMM and D-HSMM following both heat treatments. Data was recorded as the average of the cytokine ± SEM, in pg/mL. The asterisk (*) indicates a significant change.

	HSMM (pg/mL)	**D-HSMM (pg/mL)**
Acute	3.852 ± 1.570	4.337 ± 1.854
Chronic	2.166 ± 1.111	0.525 ± 0.108 *
Control	7.330 ± 1.330	9.877 ± 1.217

4.3.3 INTERLEUKIN-6

Figure 9 represents the concentration of interleukin-6 following both heat treatments. Assessing between-subject factors, a significant increase was seen by the interaction ($p = 0.0001$), treatment ($p = 0.0001$), and cell type ($p = 0.0001$). A significant difference was noted following the acute treatment on D-HSMM and the chronic treatment on D-HSMM ($p = <0.0001$). Compared to the control, the acute treatment had a significant decrease in the cytokine on HSMM ($p = 0.0012$) and D-HSMM cells ($p = <0.0001$). Following the chronic treatment, a significant difference was evident between HSMM and D-HSMM ($p = <0.0001$). Analyzing the difference between pre-treatment and post-treatment cytokine expressions, a significant change was evident in the interaction ($p = 0.0005$), treatment ($p = <0.0001$), and in the cell type ($p = <0.0001$).

Following the chronic treatment, cytokine expression between HSMM and D-HSMM was significantly different ($p = <0.0001$). The acute treatment had a significant difference between HSMM and D-HSMM ($p = 0.0005$). Following the chronic treatment, a significant increase was seen in D-HSMM ($p = <0.0001$), compared to the control. In HSMM, the concentration of IL-6 differed between acute and heat treatment ($p = 0.0030$), as well as in D-HSMM ($p = <0.0001$). Shown in Table 9, following the chronic heat treatment, D-HSMM resulted in a higher expression of IL-6. In HSMM, the expression of IL-6 following both treatments were slightly lower than the control. The concentration of cytokine expression in HSMM decreased following both treatments but had an increase in D-HSMM following the chronic treatment (Table 9).

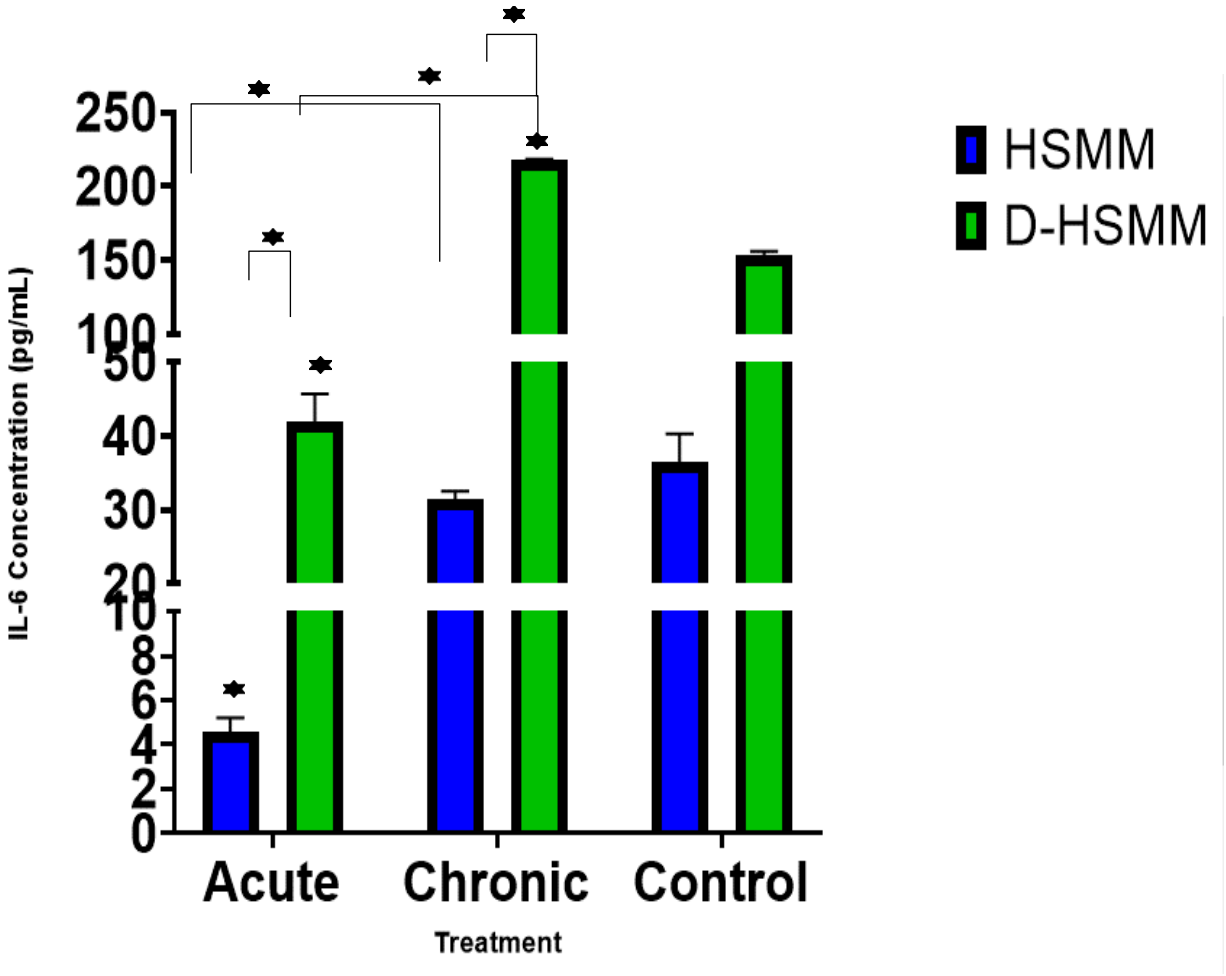

Figure 9: Concentration of IL-6 resulted in a downregulation in HSMM following both heat treatments. Additional significant downregulation of the cytokine was evident in D-HSMM following the acute treatment (p = <0.0001), while the chronic treatment yielded an overexpression(p = <0.0001) Data was recorded as pg/mL ± SEM, in pg/mL. The asterisk (*) indicates a significant change.

Table 9: The average concentration of IL-6 shows a decrease in cytokine expression in HSMM following both treatments, but an increase in D-HSMM following the chronic treatment. The data was recorded as the mean± SEM of IL-6, in pg/mL. The asterisk (*) indicates a significant change.

	HSMM (pg/mL)	**D-HSMM (pg/mL)**
Acute	4.540 ± 0.676 *	41.875 ± 3.812 *
Chronic	31.406 ± 1.120	217.991 ± 0.464 *
Control	36.390 ± 3.865	152.872 ± 3.363

4.4.4 INTERLEUKIN-10

Figure 10 outlines the cytokine expression of IL-10. Following both treatments significant change was evident in the expression of IL-10 based on the interaction ($p = 0.0036$), treatment ($p = 0.0068$), and cell type ($p = 0.0026$). Following the acute treatment, HSMM ($p = 0.0055$) yielded a significant decrease; consequently, IL-10 expression in D-HSMM also resulted in a significant decrease following the chronic treatment ($p = 0.0036$).

Assessing the significant change between IL-10 expression pre- and post-treatment, a significant change was found in interaction ($p = <0.0001$), treatment ($p = 0.0012$), and cell type ($p = 0.0003$). A significant decrease was evident in the cytokine expression of HSMM following the acute treatment ($p = <0.0001$), comparing pre-treatment and post-treatment cytokine expressions. Table 11 shows an increase in cytokine expression in D-HSMM following both treatments, but a decrease in expression in HSMM following both treatments.

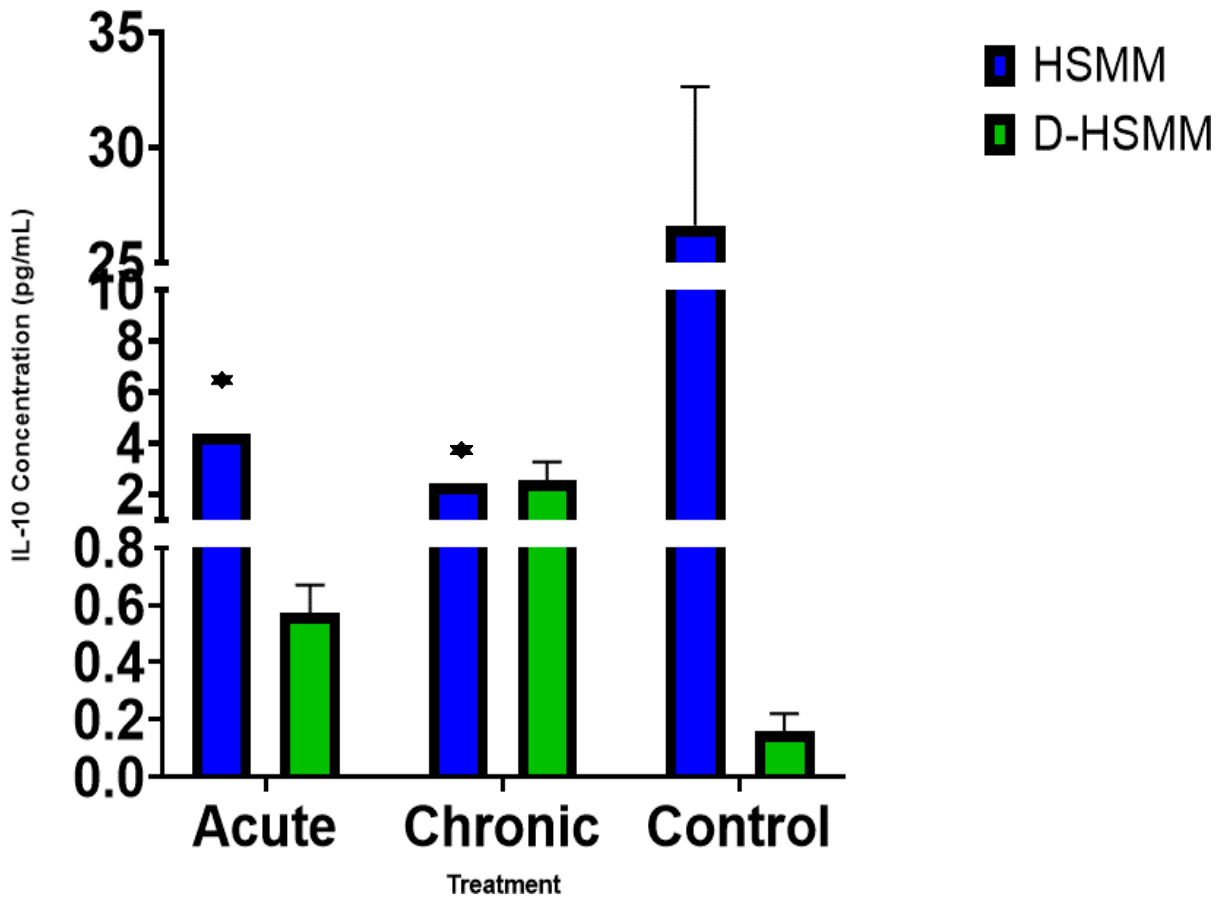

Figure 10: A significant decrease in the expression of IL-10 was evident in HSMM following the acute and chronic treatments. The cytokine was overexpressed in the D-HSMM cell line following both heat treatments. Data are expressed as average ± SEM, in pg/mL. The asterisk (*) indicates a significant change.

Table 10: The average concentration of IL-10 shows an increase in the D-HSMM following both treatments, but a decrease in expression following both treatments in HSMM. Concentration is expressed as mean ± SEM, in pg/mL. The asterisk (*) indicates a significant change.

	HSMM (pg/mL)	**D-HSMM (pg/mL)**
Acute	4.373 ± 0.000 *	0.571± 0.100
Chronic	2.443 ± 0.000 *	2.542 ± 0.743
Control	26.613 ± 6.038	0.159 ± 0.062

4.4.5 TNF-α

Following both treatments (Figure 11), both the acute and the chronic treatment had a significant change in interaction ($p = 0.0017$), treatment ($p = 0.0022$), and cell type ($p<0.001$). Following the acute treatment, a significant change was seen between HSMM and D-HSMM ($p = 0.0254$). Compared to the control, the acute treatment on HSMM also resulted in a significant change ($p = 0.0103$). A significant decrease was evident following the chronic treatment on HSMM ($p = 0.0008$), compared to the control.

Assessing within-subject factors, the cell type ($p = 0.0050$) had a significant effect on the cytokine expression. Outlined in Table 12, both acute and chronic treatments resulted in a decrease in TNF-α expression in HSMM. However, in D-HSMM, the acute treatment resulted in an up-regulation of the cytokine, while the acute treatment resulted in a decrease in the expression.

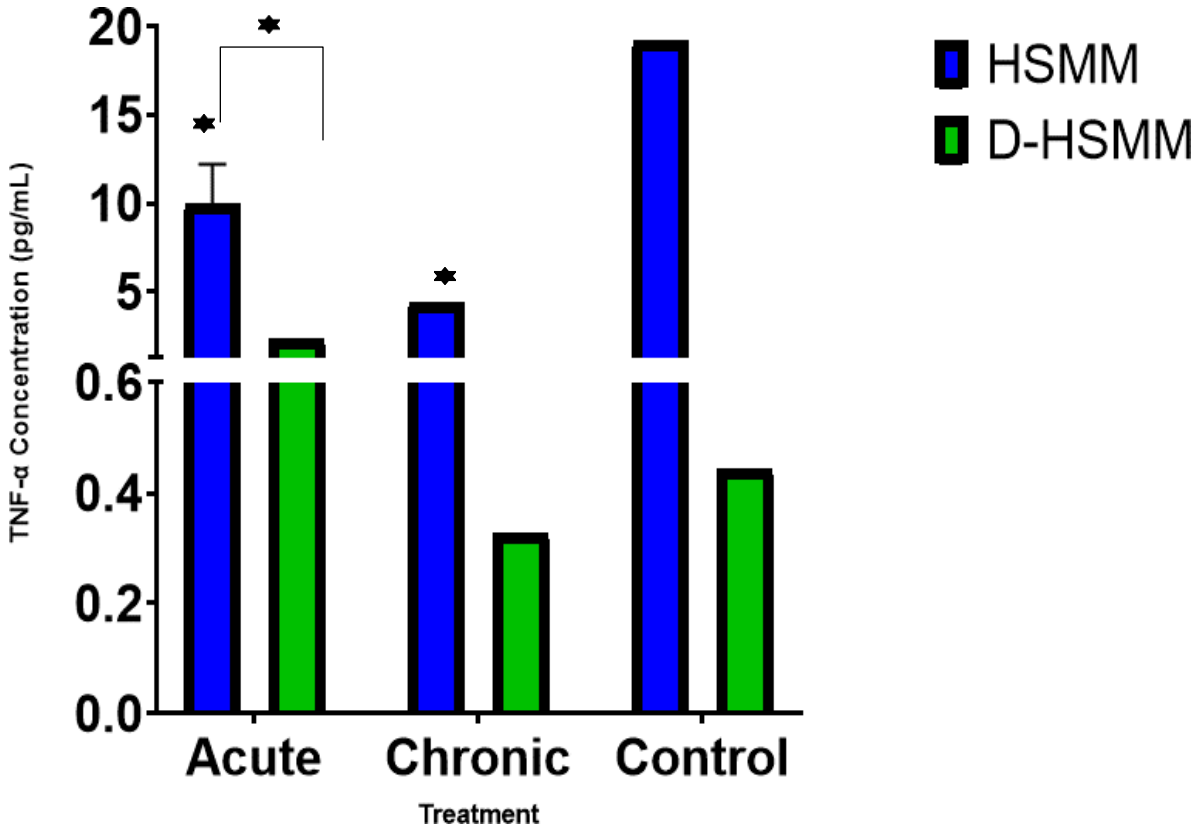

Figure 11:Both the acute and the chronic treatment had a significant change in HSMM and D-HSMM regarding the expression of TNF-α. Following the acute treatment, a significant change was seen between HSMM and D-HSMM (p = 0.0254). Compared to the control, the acute treatment on HSMM also resulted in a significant change (p = 0.0103). A significant decrease was evident following the chronic treatment on HSMM (p = 0.0008), compared to the control. Data are expressed as mean ± SEM, in pg/mL. The asterisk (*) indicates a significant change.

Table 11: A decrease is seen in HSMM following both treatments. In D-HSMM, a decrease in cytokine expression is seen following the chronic treatment, but an increase following the acute treatment. Measurements are expressed in pg/mL. The asterisk (*) indicates a significant change.

	HSMM (pg/mL)	**D-HSMM (pg/mL)**
Acute	9.977 ± 2.232 *	2.336 ± 1.775
Chronic	4.405 ± 0.000 *	0.326 ± 0.000
Control	19.213 ± 0.000	0.444 ± 0.117

5. DISCUSSION

Skeletal muscle mass reduction is evident in both diagnosed and undiagnosed Type 2 Diabetics, so it is vital to assess approaches to aid in muscle regeneration and development. Additionally, hyperthermia is known to up-regulate cytokines IL-1β, IL-6, IL-10, and TNF-α in the skeletal muscles of a mouse model[29]. The purpose of this study was to investigate the role of acute and chronic heat exposure on healthy and Type 2 Diabetic skeletal muscle myoblasts, in an in-vitro model. Factors assessed were cell density, gene expression, and inflammation.

5.1 CELL DENSITY PERCENTAGE

Cell density percentage was investigated by exposing both muscle cell types (HSMM and D-HSMM) to acute and chronic heat treatments. The goal was to determine whether the cell viability remains constant, compared to the control, when exposed to 40°C environmental temperature. The data indicates an acute exposure to an elevated temperature, 40°C, on D-HSMM, significantly decreases cell density percentage, while a chronic heat exposure on both HSMM and D-HSMM yields a higher cell density percentage. The lower density percentage expressed in D-HSMM, compared to HSMM, was expected; comparing the cell lines' Certificate of Analysis provided by the supplier, D-HSMM undergoes a longer doubling time than HSMM, 49 hours and 19 hours, respectively.

Previous studies reported distress caused by Type 2 Diabetes on muscle metabolism[40]. Outcomes of the disease on skeletal muscle include an aberrant lipid deposition and a decrease in intermyofibrillar mitochondrial content, thus impeding on the cell's response to insulin through its ability to alternate between fat and carbohydrate oxidation[40–42]. This may have influenced cell viability, wherein this study cell density percentage of D-HSMM was lower than HSMM in all treatment conditions.

Several studies using cultured muscle cells and animal models demonstrated heat stress leads to an increase in muscle protein synthesis[43–45], and increasing skeletal muscle mass[46]. This was reflected in this study, where the chronic heat exposure resulted in a higher density percentage of cell viability; HSMM was increased by 1.04-fold, while D-HSMM increased by 1.16-fold. In a human model, heat stress-associated muscle hypertrophy led to an increase in muscle strength in adult men[47,48].

It has been suggested heat stress induces muscle hypertrophy through the activation of intracellular pathways including phosphatidylinositol 3-kinase-Akt and the extracellular signal-regulated kinase[49]. The phosphatidylinositol 3-kinase-Akt pathway, activated by heat stress, inhibits the upregulation of dexamethasone-induced up-regulation of the atrophy-induced ubiquitin ligases by obstructing the FOXO transcription factor's nuclear translocation[50]. Referred to as a mitogen-activated protein kinase, the extracellular signal-regulated kinase induces gene expression in response to hypertrophic stimuli[46].

5.2 GENE EXPRESSION

An array of genes was qualitatively analyzed following each treatment. For the healthy human muscle myoblasts cell line, the top 5 genes expressed with the highest fold-change occurred after exposure to the acute treatment. However, in the diabetic human muscle myoblast cell line, the top 5 genes expressed with the highest fold-change, compared to the control, occurred mostly following the chronic treatment, except for Activin A receptor type 2B that was upregulated the most following the acute treatment. Activin A receptor type 2B (AcvR2B) was upregulated the most in HSMM and hindered in D-HSMM – 215.613 and 0.001, respectively. AcvR2B ligands myostatin and activins inhibit muscle hypertrophy[51,52]. Activins negatively affect regulators of muscle mass through its regulatory role of TFG-β[52]. An upregulation in this gene following the

acute treatment on HSMM suggests the possibility of muscle wasting which was reflected in the observed decrease of cell viability percentage following the acute treatment.

Insulin-like growth factor 2 (IGF-2) provides instructions to the cell on making IGF-2 protein, which has been shown to promote cell growth and proliferation[53]. Additionally, insulin-like growth factor 2 (IGF-2) provides instructions to the cell on making IGF-2 protein which has been shown to promote cell growth and proliferationf[53]. Such elevation suggests cell growth and proliferation in D-HSMM (Figure 5) at an elevated level following the chronic treatment, along with cell growth and development in HSMM following an acute treatment (Figure 4).

Catenin-β-1 (CTNNB1) plays a versatile role in tissue homeostasis and various human diseases. While β-catenin is a transcriptional activator, it also promotes myogenesis and growth of various tissues[54]. In cellular growth, β-catenin is identified through its recognized role as a transcription factor[55] and induction of Myc proto-oncogene protein (c-Myc) and cyclin D1[54]. This induction can occur directly or indirectly, through the paired-like homeodomain transcription factor2[54]. This indirect induction is evident in skeletal muscles exposed to in vitro stimulation of Wnt/β-cetanin[56]. Cyclin D1 and c-Myc are both transcription factors critical in cell development, proliferation, and apoptosis.

New studies indicate both transcription factors help regulate cell size[57,58]; where the overexpression of c-Myc is correlated with hypertrophy in hepatocytes and postmitotic cardiac myocytes[54,59,60]. In this study, while both HSMM and D-HSMM expressed an up-regulation of catenin-β-1, the HSMM cell line was able to express it at a higher fold. Additionally, the acute bout of 40°C resulted in a higher expression of catenin-β-1 on HSMM, which could be because a one-time exposure is a sudden change to the cell's environment, whereas, in the chronic treatment, the cells may potentially acclimate to the changes over 3 weeks.

Insulin-like growth factor-binding protein 3 (IGFBP-3) plays a critical role in the physiological function of insulin growth factor 1 (IGF-1)[61]. The expressed gene is known as the main circulating carrier of IGF-1, and the high expression in this study indicates the over activation of the IGF-1 protein. Calpain-2 (CAPN2) is part of the calcium-activated protease which plays a role in exocytosis, cell fusion, apoptosis, and proliferation[62,63]. The upregulation of CAPN2 correlates with a decrease in cell density percentage in HSMM following the acute thermotherapy, thus suggesting CAPN2 acts as an apoptotic agent following a sudden elevation in environmental temperature.

Actin-β codes for β-actin, proteins that assist in forming the structural framework inside cells[64]. Such elevation, evident following the acute treatment (Figure 5) suggests an elevation in actin activity[64] and cellular mobility responses[65,66]. Over-expression is necessary for cellular responses requiring constant and stable concentration levels[65]. This was reflected in D-HSMM following the acute treatment, indicating the one-time exposure promoted the cells to up-regulate β-actin as a response to the abrupt change in environmental temperature.

A qualitative increase in troponin T3 (TNNT3) indicates an upregulation in fast skeletal troponin T protein, part of the fast-twitch skeletal muscle[67]. Additionally, TNNT3 positively regulates the expression of Ca^{2+} channel α1 (Cav1.1)[68], where a decrease in Cav1.1 expression is associated with skeletal muscle loss[69]. In this study, the upregulation of TNTT3 in D-HSMM (0.399-fold) and HSMM (2.808-fold) following the chronic treatment may suggest an increase in the amount of Cav1.1, resulting in improved skeletal function, as reflected in the observed increase of cell viability following the chronic treatment. This also presents a new therapeutic approach for the diabetic population, where chronic thermotherapy up-regulates TNTT3 to diminish the deleterious effects of aging and disease on muscle function.

The Peroxisome Proliferator-Activated Receptor-gamma coactivator-1β (PCG-1β) encodes a protein that stimulates various transcription factors including estrogen receptor α and glucocorticoid receptor. The PCG-1β are positive regulators of skeletal muscle mass and energy metabolism[70]. An up-regulation following the chronic thermotherapy on D-HSMM suggests an increase in protein synthesis and myotube diameter. The sarcoglycan-α (SGCA) encodes a portion of the dystrophin-glycoprotein complex (DGC) which is vital in the stability of muscle fiber membranes and the linking of the actin cytoskeleton[71]. An elevation in this gene in the D-HSMM cell line suggests chronic thermotherapy up-regulates members of the DGC to protect the sarcolemma from mechanical stress in an attempt to maintain membrane integrity.

5.3 CYTOKINE EXPRESSION

Interleukin-1β and TNF-α are pro-inflammatory mediators usually referred to as external stress signals that function as indicators of organismal stress or injury in other cells[72]. IL-1β is released in response to inflammatory or infectious stimuli[73]. In previous studies, IL-1β was reported to be upregulated in an acute setting, and IL-1β was involved in the metabolic adaptation of skeletal muscle tissues as a response to noninfectious stress[73]. In this study, the concentration of IL-1β had a significant change in the cytokine expression in HSMM following the acute treatment ($p = 0.0036$) and the chronic treatment ($p = 0.0133$). The cytokine expression in D-HSMM was significantly affected during the acute treatment ($p = 0.0461$). Overall, the treatments resulted in a significant decrease in cytokine expression ($p = 0.0009$). The concentration of IL-1β decreased after the treatments, compared to the controls.

In HSMM, the cytokine expression decreased by 9.75-fold following the acute treatment, and by 3.27-fold following the chronic treatment. In D-HSMM, a decrease of 1.85-fold was seen following the acute treatment, while a decrease of 1.73-fold was noted following the chronic

treatment. The observed decrease in IL-1β expression correlates with recent studies that report a decrease in the expression of pro-inflammatory markers is associated with heat stress. This data also suggests thermotherapy may increase the levels of heat shock factor (HSF)-1 and suppress pro-inflammatory markers through competitive inhibition on NF-κB binding[74].

Overexpression of TNF-α, and IL-10, following an injury is expected and indicates normal muscle repair[29]. Following exposure of hyperthermia, however, circulating TNF-α is either delayed or lessened or completely absent[29,75–78]. In this experiment, both the acute and chronic experiments ($p = 0.0022$) resulted in a significant change in TNF-α expression in both cell lines ($p = <0.0001$): a 1.93-fold and 4.36-fold decrease in expression in HSMM following the acute and chronic treatments: a 1.36-fold decrease in D-HSMM following the chronic experiment, and a 5.26-fold increase in D-HSMM following the acute heat treatment.

Following the acute and chronic heat treatments, the expression of TNF-α in HSMM significantly decreased (acute: $p = 0.103$; chronic: $p = 0.0008$). While a decrease was also evident following the chronic heat treatment on D-HSMM, the change was not significant. However, the acute treatment ($p = 0.0254$) had a significant change between both cell types – a 1.92-fold decrease in HSMM and a 5.26-fold increase in D-HSMM.

Generally, TNF-α is a pro-inflammatory marker involved with the signaling of apoptosis and necrosis[27], through binding to the TNF receptor (TNFR)1[79]. The TNFR1 contains a C-terminal intracellular domain and utilizes signal transduction to apoptosis[79]. A down-regulation of TNF-α suggests an active cytoprotective role of HSP70[80] by recruiting HSF-1 transcription factor intracellularly and extracellularly. Our data suggest acute or chronic thermotherapy may decrease the levels of pro-inflammatory markers in skeletal muscles and thus protect cellular homeostasis.

Interleukin-4, a pleiotropic anti-inflammatory cytokine[81], is known to play various roles in homeostatic regulation and disease pathogenesis[82]. Given the concentration of IL-4 was significantly reduced following both the acute and chronic treatments ($p = 0.0043$), the results of previous studies reported an upregulation of IL-4 following strength training[81].

A decrease in cytokine expression in HSMM was noted following the acute (1.90-fold) and the chronic (3.38-fold) treatments. A decrease was also evident in D-HSMM following the acute (2.28-fold) and chronic (18.81-fold) treatments. Additionally, the decrease in D-HSMM following the chronic treatment was significant. This cytokine is known to regulate myoblast fusion with myotubes, thus promoting muscle cell fusion and growth[36] when damaged by exercise.

While there was a decrease in the cytokine expression, the acute treatment resulted in a higher concentration of IL-4 than the chronic treatment. The observed decrease in IL-4 expression may be associated with a deactivation of the humoral immune system linked to acute or chronic heat stress.

Skeletal muscle is known to produce interleukin-6 in various conditions including local muscle injury, inflammation, exercise, and hypoperfusion[83]. This pleiotropic cytokine has both anti-inflammatory and pro-inflammatory properties[84]. It is referred to as pleiotropic due to its various roles in bone metabolism, development of the neuronal and cardiovascular systems, immune and inflammatory responses, hematopoiesis, and organ development[85]. The production is usually a response to receptor-mediated signals and from disturbances in the cell's internal hemostasis[21].

Interleukin-6 attaches to its receptor through the classic or trans-signaling pathway, which is negatively regulated through suppressor cytokines including Janus kinase (JAK) and signal transducer and activator of transcription (STAT) molecules[85]. In events of inflammation, IL-6 acts

as an anti-inflammatory cytokine by directly acting on plasma cells and indirectly promoting Bcl6-dependent follicular CD4 T cell differentiation, thus promoting antibody production[85].

At temperatures above 40.5°C in humans, the translational arrest of nonessential proteins, non-HSPs, is due to the inhibition of ribosomal initiation factors[21]. Since skeletal muscle cells are capable of synthesizing and secreting IL-6 during hyperthermia, one study indicates this as IL-6 heat-shock resistance in skeletal muscles[21]. Through its role as an anti-inflammatory marker, IL-6 is capable of suppressing inflammatory responses by reducing the expression of proinflammatory cytokines TNF-α and IL-1β. Consequently, in hyperthermia, circulating levels of IL-6 and IL-10 are upregulated, while levels of TNF-α and IL-1β are absent[76], outlined in Figure 12. This was reflected in D-HSMM following the chronic treatment, where IL-6 expression was upregulated 1.43-fold.

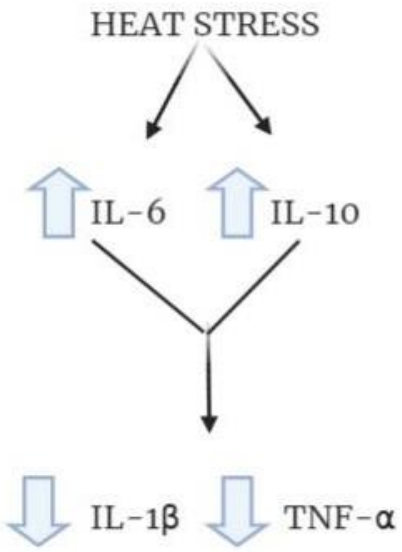

Figure 12: The expected effect of heat stress on cytokine expression. Heat-induced skeletal muscle cells anticipate an upregulation of both IL-6 and IL-10. This overexpression wILl result in an inhibition of downstream cytokines including IL-1β and TNF-α.

One explanation of IL-6 being significantly up-regulated compared to the remaining assessed interleukins is selective production of HSP could preserve the availability of other proteins involved in regulation; as evident in HSP72 inhibiting NF-$_K$B signaling, altering IL-6 regulation in LPS-induced cells[86].

The observed decrease in concentrations of IL-6 indicates a plausibility the cell lines are sensitive to insulin, which was more evident in the acute treatment group. However, the chronic treatment demonstrated an up-regulation of IL-6 ($p = <0.0001$). In relation to these findings, Welc *et al.* (2012) study reported an upregulation of IL-6 gene expression during hyperthermia in a mouse cell culture. Following acute exposure to 42°C, the expression of IL-6 was upregulated, leading to an inhibition of TNF-α mRNA[75]. The observed increase of IL-6 in the diabetic cells subjected to the chronic heat treatment may be indicative of its anti-inflammatory effect by promoting an increase in cellular viability through the reduction of inflammation, which was also observed in the downregulation of pro-inflammatory markers TNF-α and IL-1β.

Both IL-6 and IL-10 are regulated by HSF-1, where previous studies found inhibition of HSF-1 yielded an upregulation in IL-6[29]. Interleukin-10 is an anti-inflammatory cytokine, where when subjected to heat shock, can yield an early response and provide components for transcriptional messages to induce an early stress-induced immune response[29]. In this study, the expression of IL-10 had a significant change following the acute and chronic treatments ($p = 0.0068$) in both the HSMM and D-HSMM cell lines ($p = 0.0026$) – IL-10 expression was upregulated in D-HSMM following both heat treatments but was down-regulated in HSMM following the treatments.

While the change was not significant, the chronic treatment resulted in an up-regulation of the cytokine in D-HSMM, and a significant down-regulation in HSMM ($p = 0.0036$); additionally,

the acute treatment resulted in a significant decrease of the cytokine expression in HSMM ($p = 0.0055$). In D-HSMM, the cytokine was overexpressed by 3.59-fold following the acute treatment and 15.99-fold following the chronic treatment.

In HSMM, the cytokine expression decreased by 6.09-fold following the acute treatment, and by 10.89-fold following the chronic treatment. This was not expected since IL-10 was over-expressed in previous studies[75,76]. It is observed IL-10 decreased in expression in both cell lines when exposed to the heat treatments, except in D-HSMM following the chronic treatment. Such a decrease in the expression of IL-10 may be linked to the low concentrations of pro-inflammatory marker TNF-α. Similar to the report by Park *et al.* (2007), TNF-α positively correlates to the expression of IL-10 by macrophages[87]. The observed increase in the concentration of IL-10 evident following the chronic treatment on the D-HSMM cell line may benefit the cell through the prevention of the up-regulation of phagocytic and dendritic cells.

5.4 SUMMARY

The data reported here help outline inflammatory and gene regulation changes regarding thermotherapy on skeletal muscle cells. The heat exposure induced changes favoring an anti-inflammatory pathway with a decrease in the expression of IL-1β and TNF-α. The pattern cytokine expression shows the anti-inflammatory effects of IL-6 regarding suppression of IL-1β and TNF-α. Production of IL-6 protects muscle fibers from subsequent stress exposure[88]. Chronic and acute did not significantly affect the concentration of circulating cytokines IL-1β and IL-10.

In this study, IL-10 expression in D-HSMM was increased following both the acute and chronic treatments, which highlight its role as an anti-inflammatory cytokine. TNF-α expression was also decreased, except for D-HSMM exposed to the acute treatment, indicating TNF-α was suppressed by various factors including IL-6.

Chronic thermotherapy could be beneficial for the diabetic population where anti-inflammatory markers are up-regulated to maintain cellular homeostasis, and pro-inflammatory markers are down-regulated. Although a subjective tool, the gene expression array plate provided a qualitative analysis of various biomarkers applicable to the skeletal muscle cell line.

The results demonstrate skeletal muscles exhibit a different pattern of gene expression when exposed to acute treatment or chronic treatment. Additionally, these findings suggest chronic thermotherapy might improve adverse inflammatory effects associated with diabetic skeletal muscle cells.

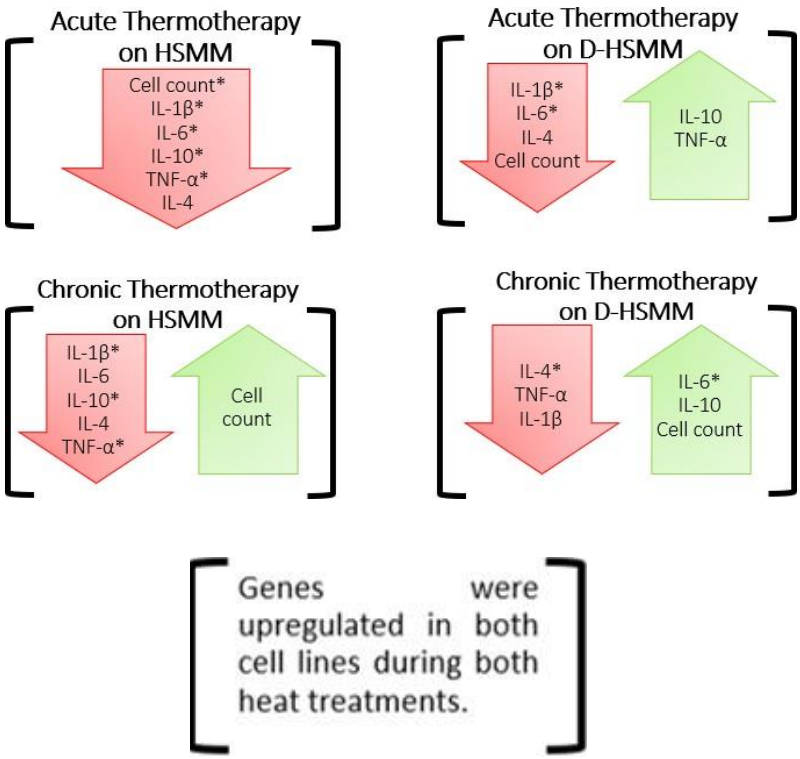

Figure 13: Summary of study results on cell density percentage, gene expression, and cytokine expression. Significant changes are marked with an asterisk (*), where p = < 0.05.

Recommendations for further study include (1) quantitatively assessing gene expression following the thermotherapies; (2) evaluating the oxidative stress of both treatments on HSMM

and D-HSMM; (3) analyzing the presence of reactive oxidative species in the cell cultures post-treatments to identify a cellular metabolic response; (4) evaluating the expression of miRNA and heat shock proteins following such treatments; and (5) assessing the effect of heat therapy on skeletal muscles in a human model.

REFERENCES

1 American Diabetes Association. Classification and Diagnosis of Diabetes: *Standards of Medical Care in Diabetes—2018*. *Diabetes Care*. 2018;41(Supplement 1):S13–S27.

2 One in Three Diabetes Fact Sheet. UCLA Center for Health Policy Research, 2014.

3 Checking Your Blood Glucose. American Diabetes Association. 2018.http://www.diabetes.org/living-with-diabetes/treatment-and-care/blood-glucose-control/checking-your-blood-glucose.html (accessed 11 Apr2019).

4 Diabetes Overview - Symptoms, Causes, Treatment. American Diabetes Association. https://www.diabetes.org/diabetes (accessed 10 Mar2020).

5 Who's at Risk? Centers for Disease Control and Prevention. 2017.https://www.cdc.gov/diabetes/basics/risk-factors.html.

6 Shaw JE, Sicree RA, Zimmet PZ. Global estimates of the prevalence of diabetes for 2010 and 2030. *Diabetes Res Clin Pract*. 2010;87(1):4–14.

7 Centers for Disease Control and Prevention. National Diabetes Statistics Report, 2020. Centers for Disease Control and Prevention, US Department of Health and Human Services: Atlanta, Georgia, 2020.

8 Scott D, de Courten B, Ebeling PR. Sarcopenia: a potential cause and consequence of type 2 diabetes in Australia's ageing population? *The Medical Journal of Australia*. 2016;205(7):329–333.

9 Yan Z, Okutsu M, Akhtar YN, Lira VA. Regulation of exercise-induced fiber type transformation, mitochondrial biogenesis, and angiogenesis in skeletal muscle. *Journal of Applied Physiology*. 2010;110(1):264–274.

10 Vienberg S, Geiger J, Madsen S, Dalgaard LT. MicroRNAs in metabolism. *Acta Physiologica*. 2017;219(2):346–361.

11 Lowell BB. Mitochondrial Dysfunction and Type 2 Diabetes. *Science*. 2005;307(5708):384–387.

12 Witzmann FA, Kim DH, Fitts RH. Hindlimb immobilization: length-tension and contractile properties of skeletal muscle. *Journal of Applied Physiology*. 1982;53(2):335–345.

13 Pedersen BK, Febbraio MA. Muscles, exercise and obesity: skeletal muscle as a secretory organ. *Nature Reviews Endocrinology*. 2012;8(8):457–465.

14 D'Souza DM, Al-Sajee D, Hawke TJ. Diabetic myopathy: impact of diabetes mellitus on skeletal muscle progenitor cells. *Front Physiol*. 2013;4:379.

15 Sinacore DR, Gulve EA. The Role of Skeletal Muscle in Glucose Transport, Glucose Homeostasis, and Insulin Resistance: Implications for Physical Therapy. *Physical Therapy*. 1993;73(12):878–891.

16 Brunt VE, Eymann TM, Francisco MA, Howard MJ, Minson CT. Passive heat therapy improves cutaneous microvascular function in sedentary humans via improved nitric oxide-dependent dilation. *Journal of Applied Physiology*. 2016;121(3):716–723.

17 Périard JD, Racinais S, Sawka MN. Adaptations and mechanisms of human heat acclimation: Applications for competitive athletes and sports: Adaptations and mechanisms of heat acclimation. *Scand J Med Sci Sports*. 2015;25:20–38.

18 Gupte AA, Bomhoff GL, Touchberry CD, Geiger PC. Acute heat treatment improves insulin-stimulated glucose uptake in aged skeletal muscle. *Journal of Applied Physiology*. 2011;110(2):451–457.

19 Hooper P. Hot-Tub Therapy for Type 2 Diabetes Mellitus. In: *The New England Journal of Medicine*. Massachusetts Medical Society, 1999, pp 917–925.

20 Racinais S, Wilson MG, Périard JD. Passive heat acclimation improves skeletal muscle contractility in humans. *American Journal of Physiology-Regulatory, Integrative and Comparative Physiology*. 2016;312(1):R101–R107.

21 Welc SS, Morse DA, Mattingly AJ, Laitano O, King MA, Clanton TL. The Impact of Hyperthermia on Receptor-Mediated Interleukin-6 Regulation in Mouse Skeletal Muscle. *PLoS ONE*. 2016;11(2):e0148927.

22 Webb P. Temperatures of skin, subcutaneous tissue, muscle and core in resting men in cold, comfortable and hot conditions. *Eur J Appl Physiol Occup Physiol*. 1992;64(5):471–476.

23 Febbraio MA, Snow RJ, Stathis CG, Hargreaves M, Carey MF. Effect of heat stress on muscle energy metabolism during exercise. *J Appl Physiol*. 1994;77(6):2827–2831.

24 Kim K, Reid BA, Casey CA et al. Effects of repeated local heat therapy on skeletal muscle structure and function in humans. *Journal of Applied Physiology*. 2020;128(3):483–492.

25 Feghali C, Wright T. Cytokines in acute and chronic inflammation. *Frontiers in Bioscience*. 1997;1(2):12–26.

26 Sultani M, Stringer AM, Bowen JM, Gibson RJ. Anti-Inflammatory Cytokines: Important Immunoregulatory Factors Contributing to Chemotherapy-Induced Gastrointestinal Mucositis. *Chemotherapy Research and Practice*. 2012;2012:1–11.

27 Idriss HT, Naismith JH. TNF alpha and the TNF receptor superfamily: structure-function relationship(s). *Microsc Res Tech*. 2000;50(3):184–195.

28 Dagdeviren S, Jung DY, Lee E et al. Altered Interleukin-10 Signaling in Skeletal Muscle Regulates Obesity-Mediated Inflammation and Insulin Resistance. *Mol Cell Biol*. 2016;36(23):2956–2966.

29 Welc SS, Clanton TL, Dineen SM, Leon LR. Heat stroke activates a stress-induced cytokine response in skeletal muscle. *Journal of Applied Physiology*. 2013;115(8):1126–1137.

30 HIRANO T. Interleukin 6 in autoimmune and inflammatory diseases: a personal memoir. *Proc Jpn Acad Ser B Phys Biol Sci*. 2010;86(7):717–730.

31 Schett G. Physiological effects of modulating the interleukin-6 axis. *Rheumatology (Oxford)*. 2018;57(suppl_2):ii43–ii50.

32 Iyer SS, Cheng G. Role of Interleukin 10 Transcriptional Regulation in Inflammation and Autoimmune Disease. *Crit Rev Immunol*. 2012;32(1):23–63.

33 Kaneko N, Kurata M, Yamamoto T, Morikawa S, Masumoto J. The role of interleukin-1 in general pathology. *Inflamm Regen*. 2019;39. doi:10.1186/s41232-019-0101-5.

34 Mantovani A, Allavena P, Sica A, Balkwill F. Cancer-related inflammation. *Nature*. 2008;454(7203):436–444.

35 Prantner D, Darville T, Sikes JD et al. Critical role for interleukin-1beta (IL-1beta) during Chlamydia muridarum genital infection and bacterial replication-independent secretion of IL-1beta in mouse macrophages. *Infect Immun*. 2009;77(12):5334–5346.

36 Horsley V, Jansen KM, Mills ST, Pavlath GK. IL-4 Acts as a Myoblast Recruitment Factor during Mammalian Muscle Growth. *Cell*. 2003;113(4):483–494.

37 Woodward EA, Prêle CM, Nicholson SE, Kolesnik TB, Hart PH. The anti-inflammatory effects of interleukin-4 are not mediated by suppressor of cytokine signalling-1 (SOCS1). *Immunology*. 2010;131(1):118–127.

38 Takii R, Inouye S, Fujimoto M et al. Heat Shock Transcription Factor 1 Inhibits Expression of IL-6 through Activating Transcription Factor 3. *JI*. 2010;184(2):1041–1048.

39 Counting cells using a hemocytometer. https://www.abcam.com/protocols/counting-cells-using-a-haemocytometer.

40 Kelley DE, Mandarino LJ. Fuel selection in human skeletal muscle in insulin resistance: a reexamination. *Diabetes*. 2000;49(5):677–683.

41 Chomentowski P, Coen PM, Radiková Z, Goodpaster BH, Toledo FGS. Skeletal muscle mitochondria in insulin resistance: differences in intermyofibrillar versus subsarcolemmal subpopulations and relationship to metabolic flexibility. *J Clin Endocrinol Metab*. 2011;96(2):494–503.

42 Nielsen J, Mogensen M, Vind BF et al. Increased subsarcolemmal lipids in type 2 diabetes: effect of training on localization of lipids, mitochondria, and glycogen in sedentary human skeletal muscle. *Am J Physiol Endocrinol Metab*. 2010;298(3):E706-713.

43 Goto K, Kojima A, Kobayashi T et al. Heat stress as a countermeasure for prevention of muscle atrophy in microgravity environment. *Japanese Journal of Aerospace and Environmental Medicine*. 2005;42:51–59.

44 Uehara K, Goto K, Kobayashi T et al. Heat-Stress Enhances Proliferative Potential in Rat Soleus Muscle. *The Japanese Journal of Physiology*. 2004;54(3):263–271.

45 Goto K, Okuyama R, Sugiyama H et al. Effects of heat stress and mechanical stretch on protein expression in cultured skeletal muscle cells. *Pflugers Arch - Eur J Physiol*. 2003;447(2):247–253.

46 Goto K, Ohno Y, Goto A et al. Some aspects of heat stress on the plasticity of skeletal muscle cells. *JPFSM*. 2012;1(2):197–204.

47 Goto K, Oda H, Morioka S et al. Skeletal muscle hypertrophy induced by low-intensity exercise with heat-stress in healthy human subjects. *Japanese Journal of Aerospace and Environmental Medicine*. 2007;44:13–16.

48 Goto K, Oda H, Kondo H et al. Responses of muscle mass, strength and gene transcripts to long-term heat stress in healthy human subjects. *Eur J Appl Physiol*. 2011;111(1):17–27.

49 Yamashita-Goto K, Ohira Y, Okuyama R et al. Heat stress facilitates stretch-induced hypertrophy of cultured muscle cells. *J Gravit Physiol*. 2002;9(1):P145-146.

50 Latres E, Amini AR, Amini AA et al. Insulin-like Growth Factor-1 (IGF-1) Inversely Regulates Atrophy-induced Genes via the Phosphatidylinositol 3-Kinase/Akt/Mammalian Target of Rapamycin (PI3K/Akt/mTOR) Pathway. *J Biol Chem*. 2005;280(4):2737–2744.

51 Hulmi JJ, Hentilä J, DeRuisseau KC et al. Effects of muscular dystrophy, exercise and blocking activin receptor IIB ligands on the unfolded protein response and oxidative stress. *Free Radical Biology and Medicine*. 2016;99:308–322.

52 Chen JL, Walton KL, Winbanks CE et al. Elevated expression of activins promotes muscle wasting and cachexia. *The FASEB Journal*. 2013;28(4):1711–1723.

53 Genetics Home Reference. IGF2 gene. U.S. National Library of Medicine, 2020https://ghr.nlm.nih.gov/gene/IGF2 (accessed 14 Mar2020).

54 Armstrong DD, Esser KA. Wnt/β-catenin signaling activates growth-control genes during overload-induced skeletal muscle hypertrophy. *American Journal of Physiology-Cell Physiology*. 2005;289(4):C853–C859.

55 Novak A, Dedhar S. Signaling through β-catenin and Lef/Tcf. *CMLS, Cell Mol Life Sci*. 1999;56(5):523–537.

56 Regulated subset of G1 growth-control genes in response to derepression by the Wnt pathway | PNAS. https://www.pnas.org/content/100/6/3245.short (accessed 2 Jun2020).

57 Piedra ME, Delgado MD, Ros MA, León J. c-Myc overexpression increases cell size and impairs cartilage differentiation during chick limb development. *Cell Growth Differ*. 2002;13(4):185–193.

58 Prober DA, Edgar BA. Growth regulation by oncogenes--new insights from model organisms. *Curr Opin Genet Dev*. 2001;11(1):19–26.

59 Kim S, Li Q, Dang CV, Lee LA. Induction of ribosomal genes and hepatocyte hypertrophy by adenovirus-mediated expression of c-Myc in vivo. *Proc Natl Acad Sci USA*. 2000;97(21):11198–11202.

60 Xiao G, Mao S, Baumgarten G et al. Inducible activation of c-Myc in adult myocardium in vivo provokes cardiac myocyte hypertrophy and reactivation of DNA synthesis. *Circ Res*. 2001;89(12):1122–1129.

61 Xin H, Zhang X, Sun D, Zhang C, Hao Y, Gu X. Chronic heat stress increases insulin-like growth factor-1(IGF-1) but does not affect IGF-binding proteins in growing pigs. *Journal of Thermal Biology*. 2018;77:122–130.

62 Huang Y, Wang KKW. The calpain family and human disease. *Trends in Molecular Medicine*. 2001;7(8):355–362.

63 Garach-Jehoshua O, Ravid A, Liberman UA, Reichrath J, Glaser T, Koren R. Upregulation of the calcium-dependent protease, calpain, during keratinocyte differentiation. *Br J Dermatol*. 1998;139(6):950–957.

64 Genetics Home Reference. ACTB gene. U.S. National Library of Medicine, 2020https://ghr.nlm.nih.gov/gene/ACTB (accessed 15 Feb2020).

65 Joseph R, Srivastava OP, Pfister RR. Downregulation of β-Actin Gene and Human Antigen R in Human Keratoconus. *Invest Ophthalmol Vis Sci*. 2012;53(7):4032–4041.

66 Bunnell TM, Burbach BJ, Shimizu Y, Ervasti JM. β-Actin specifically controls cell growth, migration, and the G-actin pool. *MBoC*. 2011;22(21):4047–4058.

67 TNNT3 Gene. Gene Cards: The Hman Gene Database. https://www.genecards.org/cgi-bin/carddisp.pl?gene=TNNT3 (accessed 14 Mar2020).

68 Pinto JR, Muller-Delp J, Chase PB. Will you still need me (Ca2+, TnT, and DHPR), will you still cleave me (calpain), when I'm 64? *Aging Cell*. 2017;16(2):202–204.

69 Delbono O, Xia J, Treves S et al. Loss of skeletal muscle strength by ablation of the sarcoplasmic reticulum protein JP45. *Proc Natl Acad Sci USA*. 2007;104(50):20108–20113.

70 Brown EL, Foletta VC, Wright CR et al. PGC-1α and PGC-1β Increase Protein Synthesis via ERRα in C2C12 Myotubes. *Front Physiol*. 2018;9. doi:10.3389/fphys.2018.01336.

71 National Center for Biotechnology Information. SGCA sarcoglycan alpha. 2020https://www.ncbi.nlm.nih.gov/gene/6442 (accessed 30 May2020).

72 Welc SS, Clanton TL. The regulation of interleukin-6 implicates skeletal muscle as an integrative stress sensor and endocrine organ. *Exp Physiol*. 2013;98(2):359–371.

73 Cannon JG, Fielding RA, Fiatarone MA, Orencole SF, Dinarello CA, Evans WJ. Increased interleukin 1 beta in human skeletal muscle after exercise. *Am J Physiol*. 1989;257(2 Pt 2):R451-455.

74 Song M, Pinsky MR, Kellum JA. Heat shock factor 1 inhibits nuclear factor–κB nuclear binding activity during endotoxin tolerance and heat shock. *Journal of Critical Care*. 2008;23(3):406–415.

75 Welc SS, Philips NA, Oca-Cossio J, Wallet SM, Chen DL, Clanton TL. Hyperthermia increases interleukin-6 in mouse skeletal muscle. *Am J Physiol, Cell Physiol*. 2012;303(4):C455-466.

76 Robins HI, Kutz M, Wiedemann GJ et al. Cytokine induction by 41.8 °C whole body hyperthermia. *Cancer Letters*. 1995;97(2):195–201.

77 Bouchama A, Ollivier V, Roberts G et al. Experimental heatstroke in baboon: analysis of the systemic inflammatory response. *Shock*. 2005;24(4):332–335.

78 Leon LR, Blaha MD, DuBose DA. Time course of cytokine, corticosterone, and tissue injury responses in mice during heat strain recovery. *Journal of Applied Physiology*. 2006;100(4):1400–1409.

79 Imao M, Nagaki M, Moriwaki H. Dual effects of heat stress on tumor necrosis factor- α -induced hepatocyte apoptosis in mice. *Laboratory Investigation*. 2006;86(9):959–967.

80 Ferat-Osorio E, Sánchez-Anaya A, Gutiérrez-Mendoza M et al. Heat shock protein 70 down-regulates the production of toll-like receptor-induced pro-inflammatory cytokines by a heat shock factor-1/constitutive heat shock element-binding factor-dependent mechanism. *Journal of Inflammation*. 2014;11(1):19.

81 Rosa Neto JC, Lira FS, Zanchi NE et al. Acute exhaustive exercise regulates IL-2, IL-4 and MyoD in skeletal muscle but not adipose tissue in rats. *Lipids in Health and Disease*. 2011;10(1):97.

82 Luzina IG, Keegan AD, Heller NM, Rook GAW, Shea-Donohue T, Atamas SP. Regulation of inflammation by interleukin-4: a review of "alternatives". *J Leukoc Biol*. 2012;92(4):753–764.

83 Luo G, Hershko DD, Robb BW, Wray CJ, Hasselgren P-O. IL-1beta stimulates IL-6 production in cultured skeletal muscle cells through activation of MAP kinase signaling pathway and NF-kappa B. *Am J Physiol Regul Integr Comp Physiol*. 2003;284(5):R1249-1254.

84 Papanicolaou DA, Wilder RL, Manolagas SC, Chrousos GP. The pathophysiologic roles of interleukin-6 in human disease. *Ann Intern Med*. 1998;128(2):127–137.

85 Murakami M, Kamimura D, Hirano T. Pleiotropy and Specificity: Insights from the Interleukin 6 Family of Cytokines. *Immunity*. 2019;50(4):812–831.

86 Chen H, Wu Y, Zhang Y et al. Hsp70 inhibits lipopolysaccharide-induced NF-κB activation by interacting with TRAF6 and inhibiting its ubiquitination. *FEBS Letters*. 2006;580(13):3145–3152.

87 Park P-H, McMullen MR, Huang H, Thakur V, Nagy LE. Short-term treatment of RAW264.7 macrophages with adiponectin increases tumor necrosis factor-alpha (TNF-alpha) expression via ERK1/2 activation and Egr-1 expression: role of TNF-alpha in adiponectin-stimulated interleukin-10 production. *J Biol Chem*. 2007;282(30):21695–21703.

88 Muñoz-Cánoves P, Scheele C, Pedersen BK, Serrano AL. Interleukin-6 myokine signaling in skeletal muscle: a double-edged sword? *FEBS J*. 2013;280(17):4131–4148.